INTERNATIONAL JOURNAL OF CLIMATOLOGY
Int. J. Climatol. **27**: 17–46 (2007)
Published online 6 July 2006 in Wiley InterScience
(www.interscience.wiley.com) DOI: 10.1002/joc.1377

RMetS
ROYAL METEOROLOGICAL SOCIETY

HISTALP – historical instrumental climatological surface time series of the Greater Alpine Region

Ingeborg Auer,[a,*] Reinhard Böhm,[a] Anita Jurkovic,[a] Wolfgang Lipa,[a] Alexander Orlik,[a] Roland Potzmann,[a] Wolfgang Schöner,[a] Markus Ungersböck,[a] Christoph Matulla,[b] Keith Briffa,[c] Phil Jones,[c] Dimitrios Efthymiadis,[c] Michele Brunetti,[d] Teresa Nanni,[d] Maurizio Maugeri,[e] Luca Mercalli,[f] Olivier Mestre,[g] Jean-Marc Moisselin,[g,] Michael Begert,[h] Gerhard Müller-Westermeier,[i] Vit Kveton,[j] Oliver Bochnicek,[k] Pavel Stastny,[k] Milan Lapin,[l] Sándor Szalai,[m] Tamás Szentimrey,[m] Tanja Cegnar,[n] Mojca Dolinar,[n] Marjana Gajic-Capka,[o] Ksenija Zaninovic,[o] Zeljko Majstorovic[p] and Elena Nieplova[q]

[a] *ZAMG-Central Institute for Meteorology and Geodynamics, Vienna, Austria*
[b] *CCRM-Climate Research Branch, Downsview, Toronto, Canada*
[c] *CRU-Climatic Research Unit, University of East Anglia, Norwich, UK*
[d] *Istituto ISAC-CNR, Bologna, Italy*
[e] *Istituto di Fisica Generale Applicata, Università di Milano, Milan, Italy*
[f] *SMI, Societá Meteorologica Italiana, Torino, Italy*
[g] *Météo France, Toulouse, France*
[h] *MeteoSwiss, Federal Office of Meteorology and Climatology, Zurich, Switzerland*
[i] *DWD-Deutscher Wetterdienst, Offenbach, Germany*
[j] *CHMI-Czech Hydrometeorological Insitute, Prague, Czech Republic*
[k] *SHMU-Slovak Hydrometeorological Institue, Bratislava, Slovakia*
[l] *Comenius University, Bratislava, Slovakia*
[m] *OMSZ-Hungarian Meteorological Service*
[n] *ARSO-Environmental Agency of the Republic of Slovenia, Ljubljana, Slovenia*
[o] *DHMZ-Meteorological and Hydrographical Service of Croatia, Zagreb, Croatia*
[p] *METEOBIH, Federal Meteorological Institute, Sarajevo, Bosnia and Herzegovina*
[q] *Bratislava, Slovakia*

Abstract:

This paper describes the HISTALP database, consisting of monthly homogenised records of temperature, pressure, precipitation, sunshine and cloudiness for the 'Greater Alpine Region' (GAR, 4–19 °E, 43–49 °N, 0–3500m asl). The longest temperature and air pressure series extend back to 1760, precipitation to 1800, cloudiness to the 1840s and sunshine to the 1880s. A systematic QC procedure has been applied to the series and a high number of inhomogeneities (more than 2500) and outliers (more than 5000) have been detected and removed. The 557 HISTALP series are kept in different data modes: original and homogenised, gap-filled and outlier corrected station mode series, grid-1 series (anomaly fields at $1^\circ \times 1^\circ$, lat × long) and Coarse Resolution Subregional (CRS) mean series according to an EOF-based regionalisation. The leading climate variability features within the GAR are discussed through selected examples and a concluding linear trend analysis for 100, 50 and 25-year subperiods for the four horizontal and two altitudinal CRSs. Among the key findings of the trend analysis is the parallel centennial decrease/increase of both temperature and air pressure in the 19th/20th century. The 20th century increase (+1.2 °C/+1.1 hPa for annual GAR-means) evolved stepwise with a first peak near 1950 and the second increase (1.3 °C/0.6hPa per 25 years) starting in the 1970s. Centennial and decadal scale temperature trends were identical for all subregions. Air pressure, sunshine and cloudiness show significant differences between low *versus* high elevations. A long-term increase of the high-elevation series relative to the low-elevation series is given for sunshine and air pressure. Of special interest is the exceptional high correlation near 0.9 between the series on mean temperature and air pressure difference (high-minus low-elevation). This, further developed via some atmospheric statics and thermodynamics, allows the creation of 'barometric temperature series' without use of the measures of temperature. They support the measured temperature trends in the region. Precipitation shows the most significant regional and seasonal differences with, e.g., remarkable opposite 20th century evolution for NW (9% increase) *versus* SE (9% decrease). Other long- and short-term features are discussed and indicate the promising potential of the new database for further analyses and applications. Copyright © 2006 Royal Meteorological Society

* Correspondence to: Ingeborg Auer, Central Institute for Meteorology and Geodynamics, Hohe Warte 38, A-1190 Wien, Austria.
E-mail: ingeborg.auer@zamg.ac.at

KEY WORDS multiple climate database; homogeneity; instrumental period; greater alpine region; gridded data sets; climate variability

Received 2 November 2005; Revised 9 May 2006; Accepted 16 May 2006

1. INTRODUCTION

The European Alps and its wider surroundings (4 to 19 °E, 43 to 49 °N, henceforth called 'Greater Alpine Region' or 'GAR') stands out through diverse climate and climate variability features in a relatively small region together with a unique long-term instrumental climate data potential. The former can be explained by the conjunction of three principal continental scale climate regimes with additional vertical effects caused by the mountain chain of the Alps. The latter is based on the existence of a number of long-term series – continuous records back to the second half of the 18th century exist for some climate elements. Thus, an effort to explore and analyse the past climate in the region's instrumental period seems worthwhile. Within its approximately 724 000 km^2 area, the GAR covers the whole territory of Switzerland, Liechtenstein, Austria, Slovenia and Croatia, together with parts of France, Germany, Italy, Czech Republic, Slovakia, Hungary, Bosnia and Herzegovina.

This paper will describe and summarise the recent status of a database developed by this group of authors with the aim to fully exploit, quality control and increase the instrumental climate data potential in the GAR. Earlier attempts started in the region during the 1990s with national level activities for some main climate elements (Böhm, 1992; Auer, 1993; Aschwanden *et al*.,1996; Bosshard, 1996; Baudenbacher, 1997; Gisler *et al*., 1997; Gajić-Čapka and Zaninović, 1997; Herzog and Müller-Westermeier, 1997; Herzog and Müller-Westermeier, 1998; Maugeri and Nanni, 1998; Buffoni *et al*., 1999; Brunetti *et al*., 2000; Szalai and Szentimrey, 2001; Begert *et al*., 2003; Likso, 2004; Begert *et al*., 2005; Zaninović and Gajić-Čapka, 2000). A comparable supranational activity was the NACD project (Frich *et al*., 1996) that focused on Northern Europe and was based on a well established collaboration within the Fennoscandian countries. Elsewhere, systematic homogenisation of climate series was undertaken mainly at the level of the national weather service (e.g. USA: Groisman and Legates, 1994; Karl *et al*., 1988; Canada: Vincent *et al*., 2002; Australia: Plummer *et al*., 1995; Spain: Brunet *et al*., 2006; and others).

It was soon realised that quality and homogeneity of long-term data were major problems that required unique solutions and lots of painstaking work. Soon after, the national homogenising activities found a common focal point in the bi- to tri-ennial 'Budapest Homogeneity Seminars' (Hungarian Meteorological Service, 1997; WMO, 1999; WMO, 2004). The two logical next steps were to extend the work to more climate elements and to reduce, as much as possible, the effects of national borders and sub-national administrative structures in the region (for respective historical details see e.g. Auer *et al*., 2005). This was performed for the first time for parts of the GAR within the ALOCLIM project (Auer *et al*., 2001).

The experience gained in the course of this project allowed a clear formulation of the basic necessities to adequately promote and support climate variability research at a regional scale in the GAR. There was the need to initiate, create and maintain a regional climate database with the following requirements:

- frictionless exchange of climate data within the region (at a higher spatial density than the already existing WMO-based CLIMAT-exchange mechanism),
- multi-parameter climate data collection (not single climate elements only),
- achievement of the best possible coverage in terms of space and time (adequate spatial resolution with respect to the spatial de-correlation distances of each climate element at a given time resolution),
- best possible extension back to the early instrumental period (data recovery and rescue from non-electronic sources),
- best possible treatment with respect to data quality (homogeneity breaks, outliers, gaps).

We believe that the time is now right to present here the first general description of this new database and provide a comparative overview on the climate variability patterns and trends in the region. Although HISTALP has already reached a certain degree of maturity, it is nevertheless a database system in development. Therefore the concluding section will discuss its current state and point towards further quantitative and qualitative improvements that are necessary and feasible to keep pace with the needs and demands emerging from climate research.

The geographical size and general concept of our initiative is positioned between a continental-to-global point of view of climate variability and local aspects based on single series studies. Therefore, this paper may not only be of regional importance but also may serve well as an example of how to fill the gap between the local-to-global scales that dominate mainstream climatic research.

2. DATA ACQUISITION AND MANAGEMENT

The leading aspects or goals for HISTALP have been mentioned already in the introduction. No limits were set *a priori* on series lengths. The early instrumental period was carefully assessed for data that had not been processed, and many additional early parts of series were recovered and digitised. Figure 1 demonstrates how station density has improved for temperature owing to the

DOI: 10.1002/joc

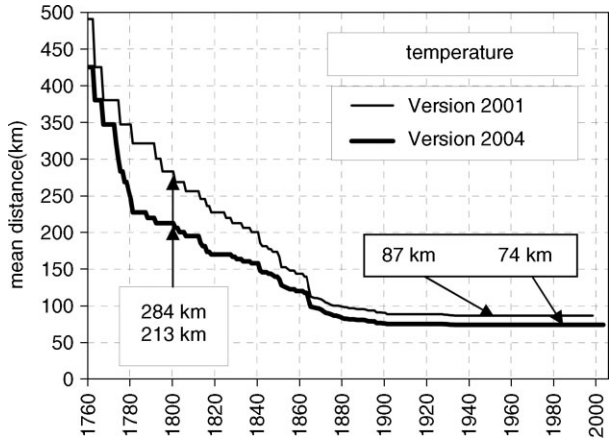

Figure 1. Network density enhancements due to HISTALP digitising and homogenising activities in recent years at the example of temperature series. Thin line: temporal evolution of mean station distance in the version used by Böhm *et al*. 2001; bold line: temporal evolution of mean station distance in the recent 2005 version.

digitising activities, particularly in the early instrumental period. This objective to improve the coverage of the early period could only be met by first accepting a compromise; owing to the fact that many original sources (regularly measured daily data) have been lost or could not be recovered, HISTALP has concentrated exclusively on monthly data, with the advantage of sophisticated possibilities for homogeneity testing and adjustment.

An interesting, but time consuming, challenge for data acquisition was and still is the political and administrative spread of the GAR and its development over the centuries. More than 30 different administrative bodies and several single-station organisations have been in charge of the HISTALP series. Many series changed nationality, the official language in which data and metadata were published and even names. The most complex examples are some sites in today's Croatia. Some older series there were started under the responsibility of the Austrian Monarchy, changed to Hungary in 1871 (the year of the foundation of an independent Hungarian Weather Service), belonged to Italy between the two world wars, became Yugoslavian afterwards and found their current authority in present day Croatia. Although it is sometimes annoying to handle this problem, it is also a good opportunity to contribute towards the further integration of a part of Europe with a complicated history. The youngest example is the recently started cooperation with the Federal Meteorological Institute of Bosnia and Herzegovina, which spatially completed the GAR in the southeast.

The backbone of our database is a subset of early series starting before 1850. All the series that are still active (or have a highly correlated neighbouring successor usable to build a compound series) were included into HISTALP. There are, however, only a few such compound series in the data set. To construct one, a correlation coefficient of at least 0.85 was assumed as the lower threshold.

In more recent times, with strongly increasing network density, only a selection of the presently available sites was used. Network density was only enhanced up to a threshold to allow for reasonable quality checks. The desirable station distance depends on the considered climate element. Typical desirable inter-station distances are, for example, 100/150 km for monthly/annual precipitation – one of the climate elements with a strong spatial de-correlation (more details in Section 5, Figures 10 and 11). These thresholds could only be surpassed for the main climate elements by the second half of the 19th century, and station density was kept constant from then on (e.g. for precipitation at ∼60 km). Only some shorter sites (in most cases high-elevation) starting later (∼1930) were additionally inserted (e.g. the highest alpine observatory on Jungfraujoch at 3580 m asl). Figures 2 and 3' show basic quantitative information about the HISTALP network.

The station map (Figure 2(a)) shows all 242 sites. The next three maps of the main elements, air pressure (b), temperature (c) and precipitation (d), represent satisfying networks in terms of the described HISTALP philosophy. Spatial distributions are homogeneous and network densities match the needs defined by spatial de-correlation. Cloudiness (e) and sunshine (f) have no data in one country each – in Italy (no sunshine data) and France (no cloudiness data). The former deficit will continue into the future (no long-term series seem to exist), the latter is due to data not yet digitised and should be solved. The strongest limitations are for the humidity elements ((g) relative humidity and (h) vapour pressure), which so far only cover parts of the GAR. They have, nevertheless, been included in this study to underline the principle of 'multiple climate'. Analyses of examples (Section 6) for the subregions shall raise awareness for future attempts to obtain data for these two climate elements.

Figure 3 shows the time-development of the HISTALP network. The differences between the thin and the bold lines illustrate the gaps in the original data. Problematic periods are the two world wars and recent difficulties due to the wars in the former Yugoslavia and the general updating difficulties for non-institutionalised international data exchange. The contrast in network density between the early instrumental period and the fully developed state (the 20th century for most elements, final maximum density of sunshine being reached even later) is clearly visible. It will be discussed later (compare the CRS-column in Table II) that the principal coarse resolution features of climate variability in the region had already been well captured in the early period (see Section 5).

3. DATA QUALITY IMPROVEMENT (INHOMOGENEITIES, OUTLIERS AND GAPS)

3.1. Homogeneity testing and homogenisation

There is general consensus that longer climatic time series do not display only pure climate variability. It is never possible to keep all aspects of the data measurement constant in time. Thus, changes in location, surroundings of sites, instruments, time of observations, observers and a number of other factors (Aguilar *et al*.,

DOI: 10.1002/joc

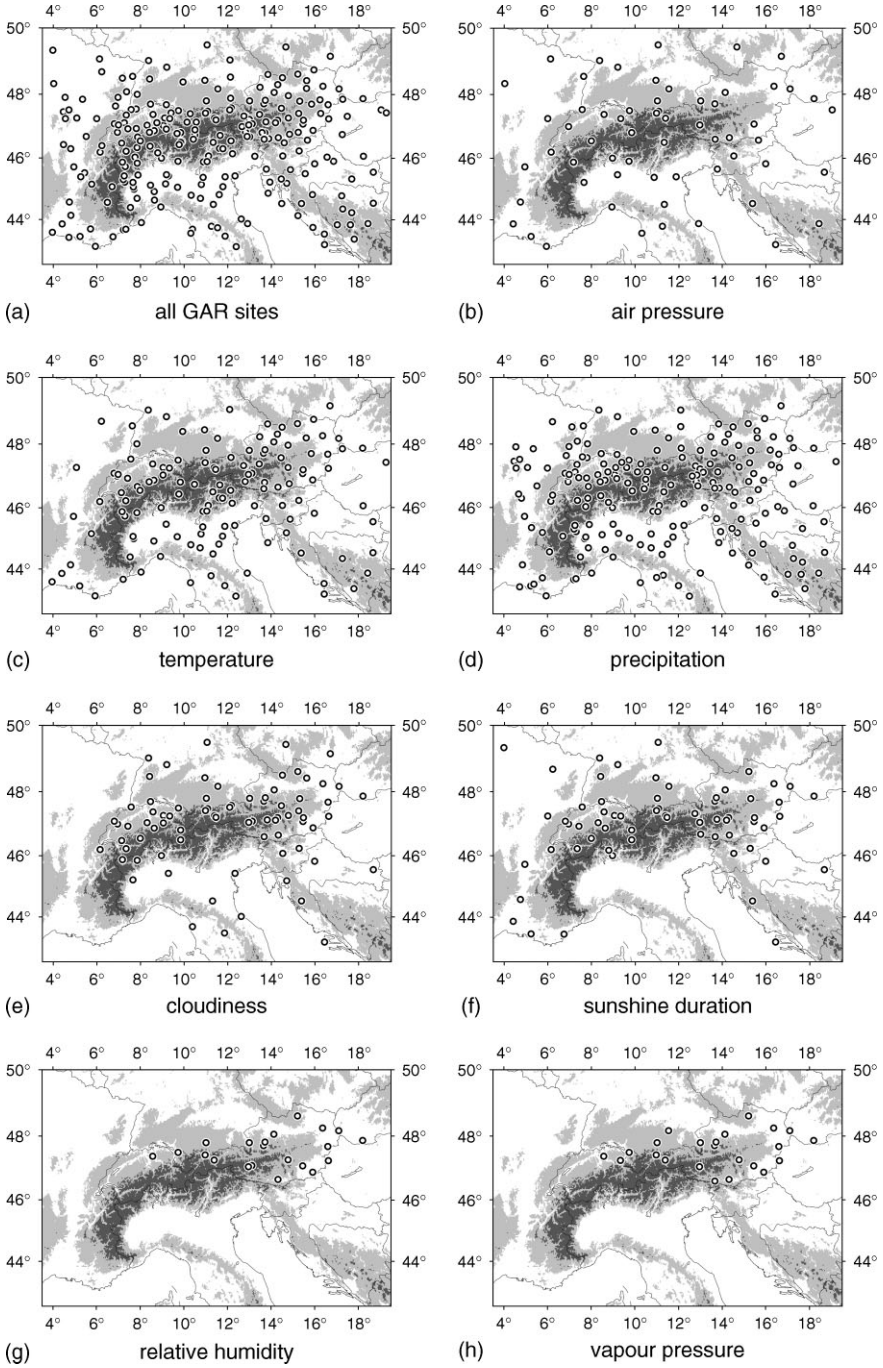

Figure 2. The GAR-networks for the climate elements: (a) any element, (b) air pressure, (c) air temperature, (d) precipitation, (e) cloudiness, (f) sunshine duration, (g) relative humidity and (h) vapour pressure. Shown are the fully developed networks typical for the 20th century.

2003; Auer *et al*., 2004; Peterson *et al*., 1998) produce inhomogeneities in the series.

As the first step of the HISTALP-QC, all the series used were subject to an intensive homogenisation procedure. We used the recent version of the HOCLIS-system, which has been described in detail using the the example of precipitation by Auer *et al*. (2005). The versions differ only marginally for other climate elements. In a nutshell, the HOCLIS concept relies on relative homogeneity testing of the series in regionally limited subgroups supported by intensive use of metadata from station histories. The size of the subgroups has to be determined by the typical spatial de-correlation of the tested climate element. No *a priori* homogeneous reference series are assumed. Each series is tested against each of the other series of a subgroup (typically ∼10 series). For the nucleus of homogeneity testing (the comparison of two series) we use Craddock's normalised accumulated difference/ratio series (Craddock, 1979), although HOCLIS would allow any method of relative homogeneity testing to be used. The practical experience in our group with a number of such methods tells us that the rejection of break signals due to statistical non-significance (as provided by higher developed methods) is often misleading.

DOI: 10.1002/joc

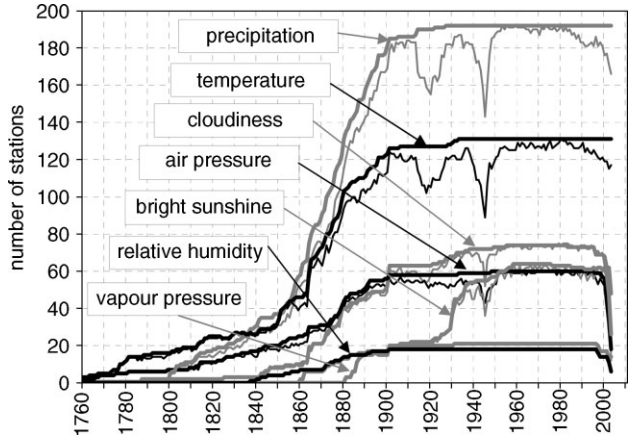

Figure 3. The development of the HISTALP station mode network of homogenised and gap-filled (bold) and original data (thin) for seven climate elements, status 2005–06.

Strong breaks may remain in the series simply owing to the fact that the typical length of a homogeneous subinterval (Table I) is short in relation to interannual variability. We try to compensate for the deficits of our method in pure statistical terms by investing much work into metadata analysis, which we regard as the ultimate measure to decide whether a break can be accepted or not. Problems arising from the shortness of some homogeneous subintervals are reduced through smoothing of the annual courses of adjustments (Auer *et al*., 2005). The resulting single break results are at first 'relative', indicating that only one of the two series has a break *versus* the other. Our initial approach does not tell us which is affected and which is not. Therefore, all the single break signals of a subgroup are arranged in a 'decision table'. In a subgroup of ten series ten such decision tables are produced, each table having one of the ten series as the tested series and the other nine as reference series. Each line of such a decision table shows the signals with one comparative series as the horizontal time-axis. If concentrations of break signals show up along vertical columns, the respective years are assumed to be the break-points (inhomogeneities) of the tested series in this decision table and are removed from the other tables of the subgroup. The rest of (scattered) the break signals are likely to appear as inhomogeneities of another series tested in another decision table. Proceeding from one decision table to the next, the ideal final result would be the assigning of all relative test signals to the respective 'most likely' affected series. Detection of mathematical breaks goes along with permanent cross-checking *versus* metadata. This is of special importance in the early period, with increasing problems in terms of the availability of nearby comparative stations. The break signals tend to become fainter in the early period, but station history in many cases still allows for a clear detection and attribution of non-climatic breaks in many cases. Another possibility to overcome the problems of low network density in the early period is 'internal homogeneity testing'. With internal testing, we compare different climate elements at one location, e.g. cloudiness *versus* sunshine duration, air pressure *versus* temperature, or any other pairs of significantly correlated climate elements. At first sight, this method seems to be a promising way to solve network density problems. Nevertheless, we strictly avoided internal testing in order to keep the series independent of information content from other elements. Thus, any future analysis of correlations, parallel trends or other similarities among different climate elements in the GAR will not be biased or affected by the process of homogenising.

The detected inhomogeneities are then adjusted, proceeding back in time from each homogeneous subperiod to the earliest one. Each adjustment is based on one comparative series best qualified in the respective subperiod and of adequate length around the break. The chosen comparative series does not necessarily have to remain the same for each subinterval. This, together with exercising great care when using remote comparative sites, helps to minimise inadmissible aligning of the series.

3.2. Outlier checks and removal of respective errors

A second step of quality control was focused on the short-term outliers in the series. For the three main elements – air pressure, air temperature and precipitation – a time consuming but effective procedure was chosen to detect and remove the errors and leave untouched those data that are exceptional but real. An interactive digital spatial intercomparison was performed for each single monthly field of the series. The procedure, histalp-05-v33.apr, is a specially designed derivate of the real-time quality control, 'GEKIS' (Potzmann, 1999), of the Austrian weather service. It displays inverse distance

Table I. Outline statistics of available data, breaks, outliers, and gaps for the five leading HISTALP elements.

	Air pressure	Temperature	Precipitation	Sunshine	Cloudiness	All	
No. of series	72	131	192	55	66	516	Series
Available data	10 215	19 312	26 063	7886	7669	71 145	Years
Mean length of the series	141,9	147,4	135,7	88,8	119,5	137,9	Years
Detected breaks	256	711	966	366	234	2533	Breaks
Mean homogeneous subinterval	31,1	22,9	22,7	11,6	26,3	23,4	Years
Detected real outliers	638	4175	529	–	–	–	Outliers
Filled gaps	4217	12 392	14 927	2011	3513	37 060	Months
Mean gap rate	3,4	5,3	4,8	2,1	3,8	4,3	%

DOI: 10.1002/joc

interpolated anomaly and absolute fields of original and homogenised data together with the measured point values. It allows for quick cross-checks between the three fields of the three climate elements. The correction estimates are visualised-near-to-real time and either immediately implemented into the HISTALP database, rejected, exchanged against another estimate or temporarily stored for closer investigation of the case. The method produces clear outlier signals for the higher spatially correlated air pressure and air temperature. For the more variable precipitation fields the procedure tended to be too critical. Subsequent queries to the data providers (who had more internal unpublished information in their archives) reduced the number of suspected values to approximately 50% of the confirmed real errors. The two screen-shots in Figure 4(a) and (b) illustrate the working facilities of histalp-05-v33.apr with the example of a 4.1 hPa error of the monthly mean air pressure of station Salzburg airport in January 1972. This case also points to the analytical potential of the database. January 1972 shows, even for the monthly mean, a strong +8 hPa W–E gradient of air pressure anomalies in the GAR, which resulted in a pronounced southerly air flow and the corresponding consequence of a dynamic lee trough north of the Alps (which would have been partly destroyed by the Salzburg-outlier in the original data). Finally, the third map (Figure 4(c)) provides the respective high-resolution precipitation field (Efthymiadis *et al.*, 2006) with the typical orographical enhancements in the south (up to 400 mm) and the dry situation (down to 0 mm) in the north.

A second class of apparent outliers was classified as 'overshooting' adjustments. Overshooting can happen when the respective homogeneous subperiod is too short to produce robust samples to apply the general adjustment philosophy, which is based on the assumption of temporally constant differences (ratios) of two highly correlated climate series. One way to avoid this is to neglect the detection signals for intervals that are too short. This way of 'soft homogenising' leaves detected and sometimes even strong inhomogeneities as they are. We did not follow this path, but tried to adjust shorter sub-periods as well and re-adjusted those with the 'overshooting' tendency during the subsequent outlier detection and elimination.

It can be argued, in general, that non-detected outliers could have a feedback on the calculation of adjustments and that erroneous outliers should be removed before starting to homogenise. On the other hand, our practical experience on thousands of analysed monthly fields of original, homogenised, anomaly and absolute temperature, precipitation and air pressure, revealed that such feedback also exist the other way round. Non-homogenised breaks can affect the detection and adjustment of erroneous outliers as well. So our solution was to

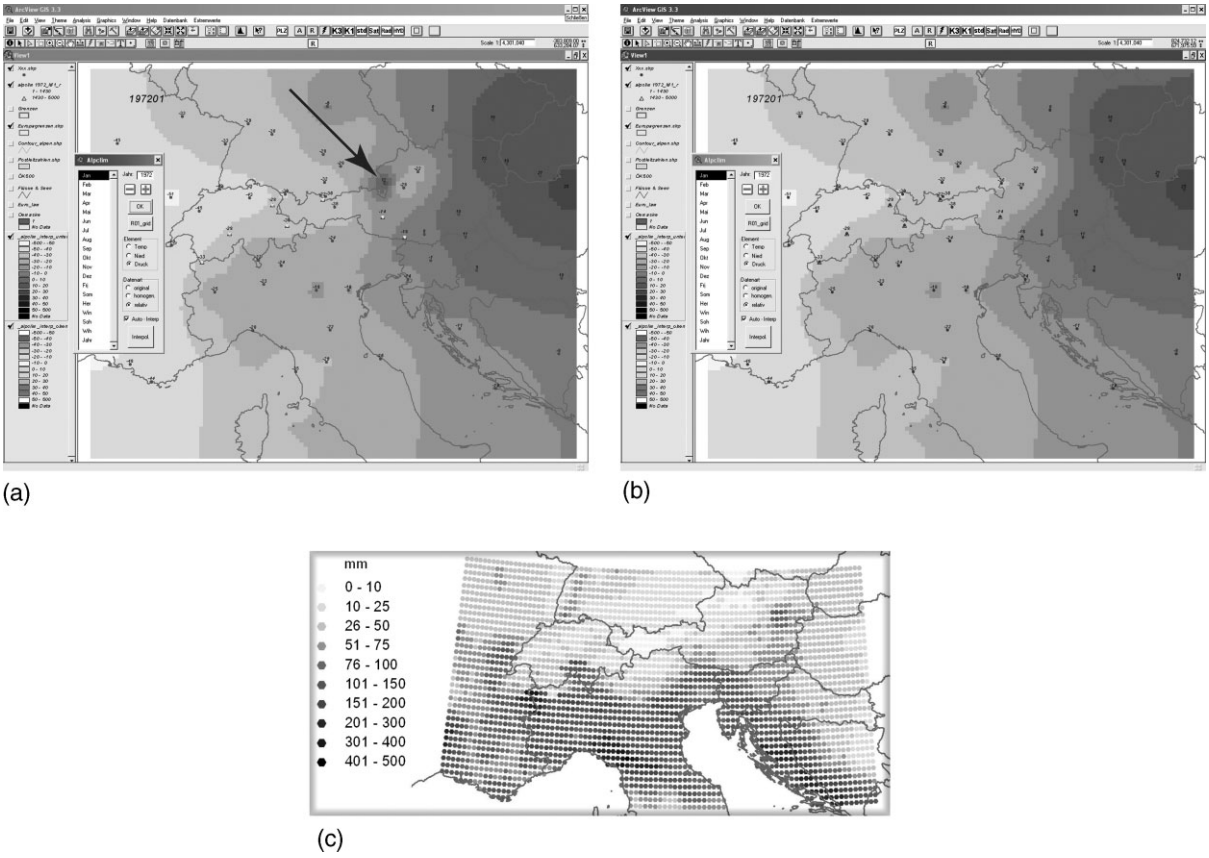

Figure 4. Screen-shots of two situations in the course of applications of the outlier detection and correction procedure, histalp-05-v33.apr. Shown are the air pressure anomaly fields in the GAR for January 1972 (a) before and (b) after correcting the respective monthly mean of airport station Salzburg (indicated by an arrow) by 4.1 hPa and (c) the respective high-resolution (R01-grid-2) precipitation field.

DOI: 10.1002/joc

conform to the described way of proceeding (homogenising, outliers, gaps) but to reduce the possible biases in feedback in two ways.

Firstly, we tried to eliminate larger outliers in advance. For this we applied the procedure described below on the original series (serial cross-checks with regional means), for the series on cloudiness and sunshine. Secondly, the fact that we smooth the annual course of break-adjustments (details in Auer *et al*., 2005) reduces the feedback biases, particularly where it is expected to be most severe – between the two breaks in the case of short intervals (compare the arguments on statistical significance in homogeneity testing in Section 3.1).

For the two other climate elements with near complete spatial coverage (cloudiness, sunshine), outlier detection was done in a more conventional way. Seasonal series were cross-checked against the respective subregional mean series. This time-saving method is able to detect serious outliers but does not have the same detection power as the procedure applied to the three main elements. The two humidity elements (relative humidity, vapour pressure) are only homogenised and not outlier corrected even now. This will be done when future projects provide the necessary personnel and resources to complete their spatial coverage for the entire GAR.

Separate internal evaluations have already shown that the work invested so far in outlier elimination has not changed the leading patterns and magnitudes of longer-term climate trends in the region. The area of application for which a remarkable increase in quality could be achieved is the analysis of any kind of extreme events. Many of the outliers that were removed would have significantly influenced (increased) the frequency and magnitude of the extreme climate events in the region. Therefore, the HISTALP database in its present state can also be described as usable for extreme event analysis on a one-month time resolution for the three main elements and a one-season resolution for sunshine and cloudiness.

3.3. Data gap filling

The final step in data processing does not deal with data quality but with completing the series. Up to a certain length, gaps were filled using the most suitable (highest correlated) nearby series. We defined no obligatory size threshold for which a gap should be filled. This question was handled flexibly, optimising the importance of a series for the database *versus* the length of the gap. Anyway, gaps of more than ten years were closed only in very rare cases and only in the early period. For applications sensitive to spatial information, the original series (with gaps) were kept in the database. It should be stressed that any gap filling should be done at the final step of data processing. This avoids the possible use of error affected comparative series for gap filling, which could duplicate or multiply the occurrence of an eventual inhomogeneity or outlier in the database.

3.4. Overall results from all quality improvements

Table I and Figure 5 outline and summarise a quantitative analysis of what has been changed through the process of quality enhancement of the five leading climate elements in HISTALP. The fact that a total of 2533 breaks could be detected and removed in the 516 time series of the five climate elements with GAR coverage underlines the necessity to work exclusively with homogenised data if the sample exceeds the average length of a homogeneous subinterval, which is little more than 20 years. To achieve statistical significance in trend or variability studies, the relatively strong and typical interannual variability of climate series strictly demands samples that are explicitly longer than that. The bold lines of the mean difference series 'homogenised minus original' in Figure 5 deviate from zero for several climate elements over longer periods. This indicates that the total of all inhomogeneities in the GAR tends to be not random but systematic. These biases are not significant in statistical terms but some of them are of an order comparable to respective long-term global climate trends. In the case of temperature, for example, the centennial trend from the 1870s to the 1980s in the original series is biased by half a degree C – the reasons for this are given in Böhm *et al.* (2001). It is a combined effect of the trend of decreasing urbanness for the typical GAR long-term series in the 20th century, together with some systematic changes in the time of observation. The remarkable early bias of original precipitation data by approximately −10% could be explained by Auer *et al*. (2005) through the systematically higher installation of rain gauges in the early instrumental period.

There is evidence that such systematic biases in climate data sets will continue to occur into the future. Even under the strictest observance of regulations they are sometimes inevitable. One such evolution is happening right now – automation of the meteorological networks. It is hoped that such biases will be detected and, hopefully, adjusted in the near future, when long enough comparative series will be available.

The broad range of individual breaks is visualised in Figure 5 by the grey lines, which define the standard deviation values of all applied adjustments. This gives the typical deviation of a single series from the climatic truth. This range is about 3 to 5 hPa for air pressure, 2 °C for temperature, 20% for precipitation, 10 to 15% for sunshine duration and 10% for sky cloudiness coverage. The even broader total range of all individual HOM-ORI differences (the thin black lines in Figure 5) also reflects the detected outliers in the original series. Taking into account that only the annual means are shown here, which smooth the real single monthly outliers, there should be no question that studies on climate extremes and their trends must strictly remain within the data purview of accurately outlier corrected series. Even with a climate element like air pressure, which is always regarded as essential and therefore treated with great care, outliers are still present.

DOI: 10.1002/joc

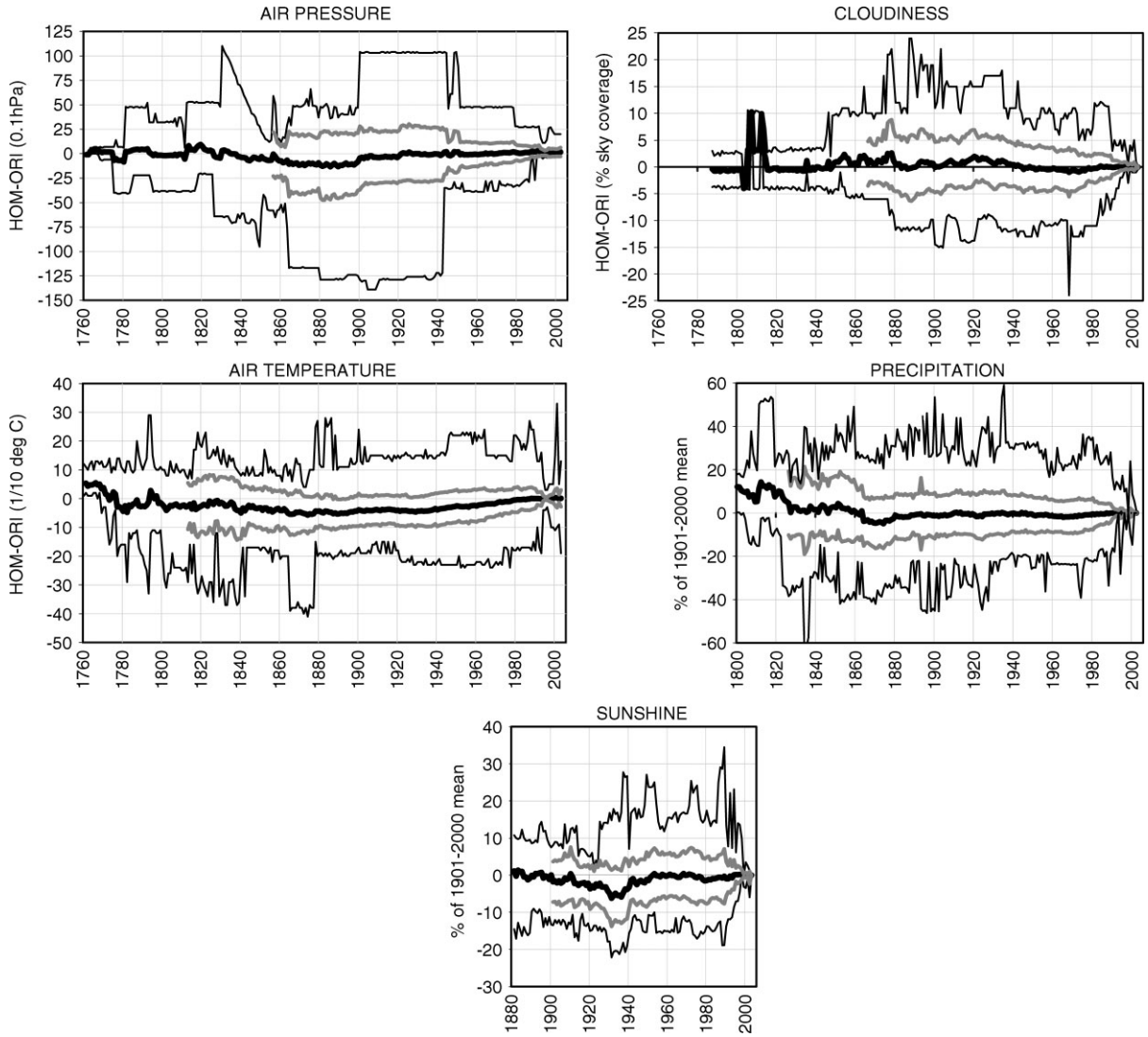

Figure 5. Annual HOM-ORI series of the five main climate elements present in the HISTALP database. ORI (original series), HOM (series after homogenisation and outlier correction). Bold black: mean difference HOM-ORI. Medium grey: 1 standard deviation range. Thin black: total range.

Figure 6 summarises and quantifies what has been said about outliers and gaps for the three main climate elements. The time series of outlier rates (figures on the left) indicate more about internal system stability of meteorological networks while the gap rates (figures on the right) seem to react more to external influences. Considering the better detectability of outliers in air pressure and air temperature series (due to their smoother monthly anomaly fields), the lower outlier rate for precipitation may not be a measure of higher quality but rather an expression of still hidden outliers in the more variable anomaly fields. The smaller number of outliers in air pressure data compared to temperature may well indicate real quality differences. The low outlier rates of air pressure before 1820 is certainly not an indicator of better quality but arises from the very low number of early series that had remained to allow for reasonable detection. For temperature, the respective network densities are better for the early period, showing that the pre-1820 series are at least as outlier affected as they were afterwards. Variable detectability does not play any role for the gap rates of the series shown in the right side panels of Figure 6. Rates are similar for the three climate elements and obviously more strongly influenced by external factors. The two World Wars are clearly visible with peaks in gap rates up to 25%. The typical gap rates in politically calm periods of the 'IMO-WMO period' are between 1 and 5%. The fact that they are zero only in very rare cases underlines the great benefit of gap filling for any application. The pre-IMO period has considerably increased gap rates, which are lower only in the very early centuries of the instrumental period. Here, the few remaining classical astronomical observatories seem to have had a higher level of staying power than the early attempts to install networks. This introduced a greater number of new series but also brought in more instability.

DOI: 10.1002/joc

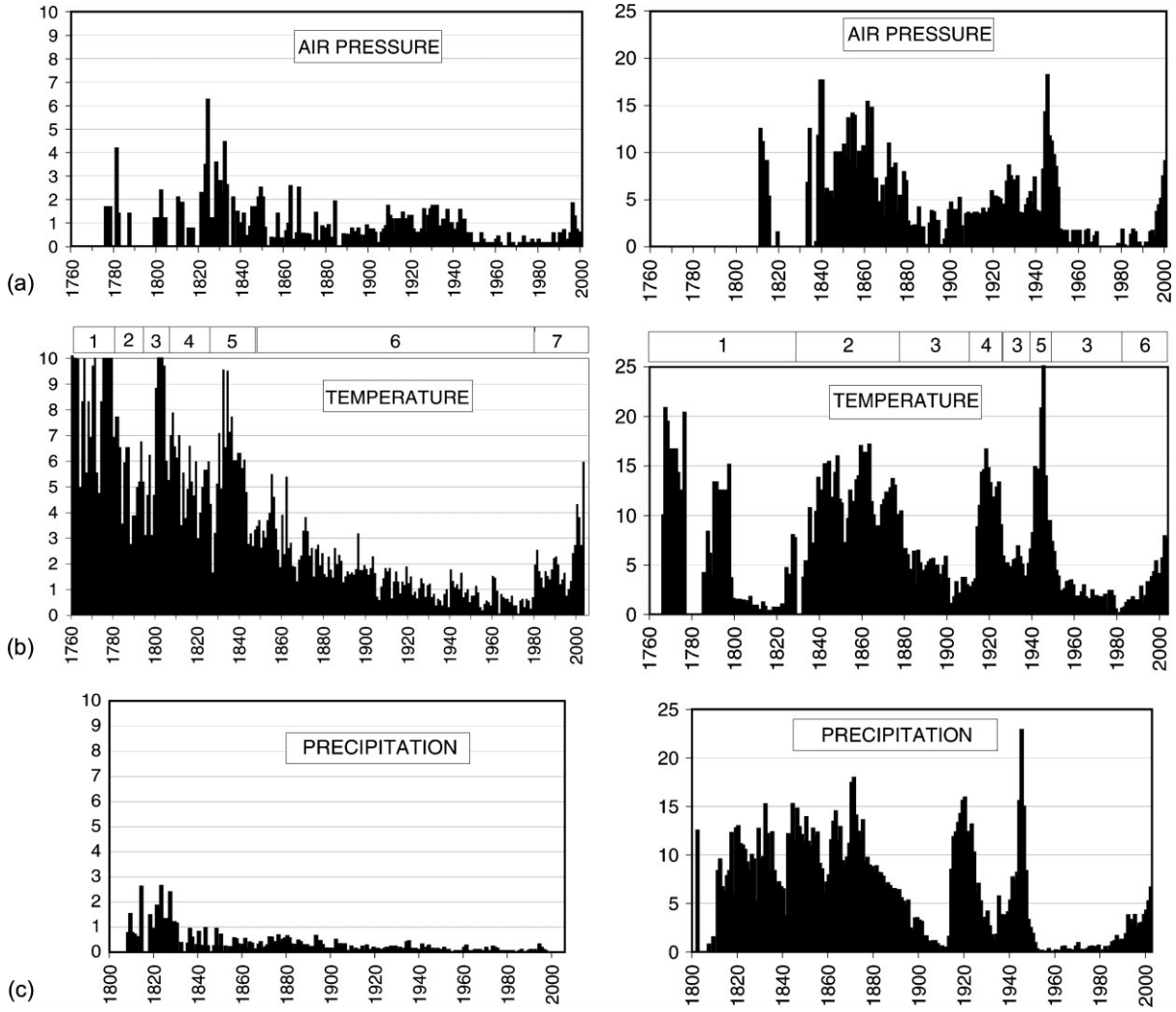

Figure 6. Time series of outlier rates (left panels) and gap rates (right panels) in the HISTALP series of (a) air pressure, (b) air temperature and (c) precipitation. Outlier and gap rates in percentage (in relation to the amount of available data). Historical periods in (b) left panel: 1, early observatories; 2, *societas meteorological palatina* network; 3, Napoleonic wars; 4, recovery of the *palatina* network; 5, new early regional networks; 6, stable period of meteorological services; 7, recent problems in the Italian network and the network of Bosnia and Herzegovina, in (b) right panel: 1, early period; 2, first networks with continuity problems; 3, well organised IMO period; 4, World War I; 5, World War II; 6, recent problems in the Italian network and the network of Bosnia and Herzegovina.

4. HISTALP DATA MODES

Table II provides an overview of the sites that best represent the HISTALP philosophy. They are prominent in terms of being 'multiple' and 'long' or belonging to the summit station subset, which allows study of the third dimension of climate variability in the region. The following sections will provide a first comparative outline of the leading climate variability features in the GAR on the basis of the concept of 'Coarse Resolution Subregional Means' (CRSMs). Column CRS in Table II gives the results of the regionalisation discussed in the next section.

The climate information in HISTALP is stored in station mode and grid mode. The former provides two kinds of data: 'stmod-ori' (monthly/seasonal/annual means or totals of the original data) and the subsequent 'stmod-hom' data. Stmod-hom series have passed the homogeneity tests, outlier correction and gap filling procedures. The current stmod part is presented by the maps in Figure 2.

Three climate elements, air pressure means (P01), air temperature means (T01) and precipitation totals (R01) have been also transferred into monthly anomaly fields (with respect to 1901–2000 averages) at a grid resolution of 1° latitude and longitude. These 'grid-1' series will reduce the remaining undetected inhomogeneities/outliers through the process of averaging, overcome any remaining inhomogeneities of the network in terms of spatial distribution of the sites and allow for easier mathematical treatment in different kinds of analyses. The method applied was a modified Gaussian weighted inverse distance (IDW) interpolation. The filter width of the weighting function was set with respect to spatial de-correlation of the respective climate element (least for precipitation, largest for air pressure). A few steep climate gradients in the Alpine main chain for all elements, coastal *versus* inland for temperature and a few others, were initially

DOI: 10.1002/joc

Table II. List of 66 outstanding HISTALP sites from the whole sample of 242. Selection criteria: multiple with at least four elements and beginning before 1850; summit site: multiple with at least 3 elements, or starting before 1800. Column CRS refers to the attribution of elements to the respective 'coarse resolution subregion' (details in Chapter 5).

Station identification		Coordinates			CRS	Starting years of the series						
Full name	Nat	Long	Lat	Alt		P01	T01	R01	SU1	N01	H01	H11
	Recent nationality	Degree E	Degree N	M above sea level	Coarse resolution subregion	Air pressure means	Temperature means	Precipitation totals	Sunshine duration totals	cloudiness	Relative humidity means	Vapour pressure means
Augsburg	DE	10.93	48.42	463	1	1812	1813	1812	1947	1901	–	–
Bad Gleichenberg	AT	15.90	46.87	280	1	–	1880	1879	1930	1879	1878	1878
Bad Ischl	AT	13.63	47.72	512	1	1855	1855	1858	1880	1864	1860	1860
Badgastein	AT	13.12	47.09	1100	1	–	1854	1858	–	1864	1913	–
Bratislava	SK	17.10	48.17	280	1	1852	1850	1857	1934	1872	1871	1871
Brno	CZ	16.70	49.16	241	1	1851	1848	1805	–	1871	–	–
Budapest	HU	19.22	47.45	130	1	1809	1780	1841	–	–	–	–
Graz	AT	15.45	47.08	377	1	1837	1837	1837	1922	1864	1862	1856
Hohenpeißenberg	DE	11.02	47.80	986	1	1781	1781	1800	1937	1879	1879	1880
Hurbanovo	SK	18.20	47.87	124	1	1874	1872	1871	1934	1872	1872	1872
Kremsmünster	AT	14.13	48.05	389	1	1822	1767	1820	1884	1842	1862	1840
München	DE	11.55	48.18	525	1	1825	1781	1848	1936	1825	–	1842
Osijek	HR	18.67	45.55	91	1	1899	1899	1899	1957	1899	–	–
Regensburg	DE	12.10	49.03	366	1	–	1773	1800	–	–	–	–
Salzburg	AT	13.00	47.80	430	1	1842	1842	1839	–	1842	1862	1853
Sopron	HU	16.60	47.68	234	1	–	1871	1865	1929	1871	1872	1872
Stift Zwettl	AT	15.20	48.62	505	1	–	1883	1883	1930	1883	1883	1883
Szombathely	HU	16.63	47.27	221	1	–	1874	1865	1929	1873	1876	1876
Wien	AT	16.35	48.22	209	1	1775	1775	1841	1881	1842	1862	1837
Altdorf	CH	8.63	46.87	449	2	–	1864	1864	1956	1864	–	–
Basel	CH	7.60	47.60	316	2	1760	1760	1861	1886	1864	–	–
Bern	CH	7.42	46.93	565	2	–	1777	1856	1886	1901	–	–
Bregenz	AT	9.73	47.50	424	2	1874	1869	1874	–	1872	1873	1873
Davos	CH	9.84	46.81	1590	2	1901	1866	–	1886	1901	–	–
Feldkirch	AT	9.62	47.27	440	2	–	1875	1876	1936	1878	–	–
Genève	CH	6.15	46.19	380	2	1768	1760	1826	1901	1846	–	–
Innsbruck	AT	11.38	47.27	609	2	1830	1777	1858	1906	1866	1883	1893
Karlsruhe	DE	8.35	49.03	112	2	1868	1779	1801	1936	1880	–	–
La Chaux-de-Fonds	CH	6.80	47.09	1018	2	–	1900	1900	1901	1901	–	–

DOI: 10.1002/joc

Lyon	FR	4.94	45.72	198	2	1881	1851	1841	1881	–	–	–
Neuchatel	CH	6.95	47.00	485	2	1864	1864	1856	1901	1901	–	–
Sion	CH	7.37	46.23	482	2	–	1864	1861	1941	1864	–	–
Strasbourg	FR	7.64	48.55	150	2	1892	1801	1803	–	–	–	–
Stuttgart	DE	9.20	48.83	311	2	1826	1792	1807	1925	1900	–	–
Zürich	CH	8.57	47.38	556	2	1864	1830	1830	1886	1864	1901	1901
Celje	SI	15.27	46.23	234	3	–	1851	1853	1950	1932	–	–
Gospic	HR	15.38	44.53	573	3	1872	1872	1873	1957	1872	–	–
Hvar	HR	16.43	43.17	20	3	1858	1858	1858	1952	1858	–	–
Klagenfurt–Flughafen	AT	14.33	46.65	459	3	1844	1813	1813	1884	1844	1860	1845
Ljubljana	SI	14.52	46.07	316	3	1854	1851	1853	1948	1891	–	–
Padova	IT	11.88	45.40	14	3	1766	1774	1800	–	–	–	–
Pèsaro	IT	12.91	43.87	11	3	1879	1871	1866	–	–	–	–
Sarajewo	BA	18.43	43.87	630	3	1880	1880	1880	–	–	–	–
Trieste	IT	13.77	45.65	67	3	1841	1841	1841	–	–	–	–
Venezia	IT	12.33	45.43	1	3	–	1868	1836	–	1900	–	–
Zagreb	HR	15.98	45.82	162	3	1862	1861	1862	1889	1861	–	–
Bologna	IT	11.34	44.45	60	4	1814	1814	1813	–	1879	–	–
Bozen/Bolzano	IT	11.33	46.50	272	4	1878	1850	1856	–	–	–	–
Firenze	IT	11.25	43.78	75	4	1814	1878	1860	–	–	–	–
Genova	IT	8.93	44.42	53	4	1833	1833	1833	–	–	–	–
Lugano	CH	8.97	46.00	273	4	1864	1864	1861	1886	1864	–	–
Marseille	FR	5.23	43.44	5	4	1883	1847	1800	1930	–	–	–
Milano	IT	9.19	45.47	103	4	1763	1763	1800	–	1763	–	–
Torino	IT	7.67	45.07	275	4	1799	1760	1803	–	1787	–	–
Toulon	FR	5.93	43.11	24	4	1891	1891	1870	–	–	–	–
Verona	IT	10.87	45.38	67	4	1880	1788	–	–	–	–	–
Feuerkogel	AT	13.72	47.82	1618	5	–	1930	–	1930	1930	1931	1931
Gr. St Bernhard	CH	7.18	45.87	2472	5	1864	1818	–	–	1846	–	–
Jungfraujoch	CH	7.98	46.55	3580	5	1933	1933	–	1931	1938	–	–
Patscherkofel	AT	11.46	47.21	2247	5	–	1931	–	1935	1932	–	–
Säntis	CH	9.35	47.25	2490	5	1883	1864	–	1888	1882	–	1901
Schmittenhöhe	AT	12.73	47.33	1973	5	–	1880	–	1929	–	–	–
Schöckl	AT	15.47	47.20	1445	5	–	1901	–	1929	1929	–	–
Sonnblick	AT	12.95	47.05	3105	5	1887	1886	–	1887	1887	1887	1886
Villacher Alpe	AT	13.67	46.60	2160	5	1880	1851	–	1884	1878	–	1880
Zugspitze	DE	10.98	47.42	2962	5	1900	1901	–	1900	1901	1900	1901

Int. J. Climatol. **27**: 17–46 (2007)
DOI: 10.1002/joc

defined as barriers to information transport. Also, the search radius was set according to the specific spatial decorrelation. This was a measure to avoid transfer of information to a grid point over unrealistically long distances, especially in the earlier times when network density was less. For temperature, two such grid-1 data sets were produced. The version 'high-elevation' is only present for grid points in the direct Alpine realm and was calculated from a selection of high-elevation or summit series (comp. Table II). The version 'low-elevation' comprises all grid points in the GAR from 4 to 19 °E and 43 to 49 °N. For precipitation, the series from the wind exposed summit sites have already been excluded from the stmod data set (Auer *et al*., 2005) owing to the well known uncertainties of precipitation measurements at high-elevation Alpine sites (Sevruk, 1986; Milković, 1989; Auer, 1992; Yang *et al*., 1999a, 1999b; Forland and Hanssen–Bauer, 2000; Milković, 2002), consequently, no high-elevation grid-1 version was produced. For air pressure, only sites up to a maximum altitude of 650 m asl were used for grid point-interpolation. These low-elevation fields can be expected to carry the main information usable for questions of circulation. Higher-elevation sites were excluded owing to their systematic bias originating from the temperature and humidity of the atmospheric layers beneath. However, studies targeting such effects directly remain in the low- and high-elevation pairs of the stmod series (e.g. Böhm *et al*., 1998).

At present, a second kind of a gridded data set has also been produced for precipitation. R01-grid-2 consists of absolute monthly precipitation totals at a high spatial resolution of 1°/6° lat/long. Efthymiadis *et al*., 2006 describe the procedure in detail. The high-resolution data set is principally based on two main sources. The HISTALP stmod-hom data set provides the long-term information back to 1800. It has been merged with the shorter (1971–1990) but higher resolved ETHZ-precipitation climatology (Schwarb, 2000; Schwarb *et al*., 2001). The basic assumption is the relative stability of the (highly resolved) ETHZ-patterns of spatial variability allowing the statistically-sophisticated extension back in time via the (spatially less resolved) HISTALP stmod data.

As the example of a 19th century subset of a precipitation series, Freiburg in southern Germany (Figure 7) provides a comparison of the four data modes (stmod-ori, stmod-hom, R01-grid-1 and R01-grid-2). Before 1869 (the start of the Freiburg precipitation series), only interpolated grid series were available – in mm for grid-2, in percent of the 20th century mean for grid-1. The systematically lower grid-2 series compared to stmod-hom are typical for this case, which highlights extremes and not the average situation. It can be explained by the location of Freiburg in a steep W–E gradient of increasing terrain (Schwarzwald) with increasing precipitation. The nearest grid-2 series is, in spite of the high resolution of grid-2, representative of the lower, drier Rhine valley to the West (7.75 °E and 47.92 °N).

5. REGIONALISATION – THE CONCEPT OF COARSE RESOLUTION SUBREGIONS

This paper intends not only to describe the acquisition, quality enhancement and general structure of the HISTALP database but also to give a first survey of the general climate variability features in the region. It is clear that there have been significantly different short- and long-term climate evolutions in the GAR (e.g. for precipitation, as described by Brunetti *et al*., 2005). Therefore, it was necessary to reduce the number of local-to-subregional differences, from element to element and from subperiod to subperiod, to some principal features.

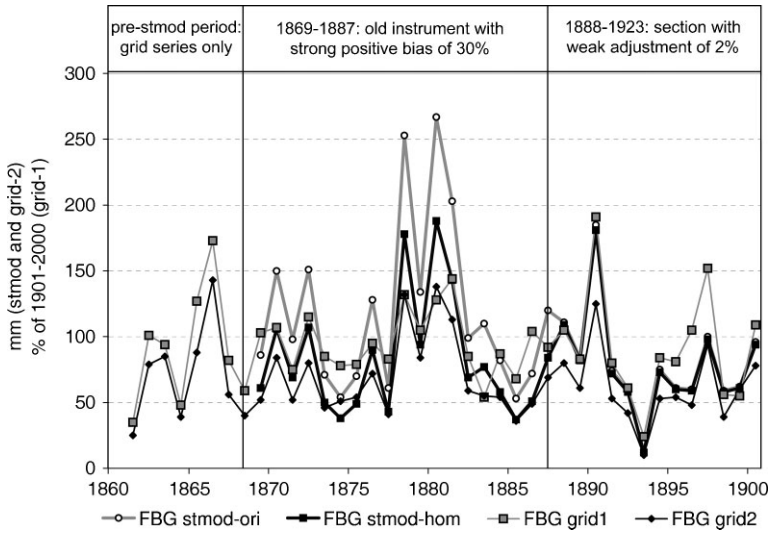

Figure 7. Example for the four different kinds of time series available in HISTALP: Freiburg/Breisgau, Germany, August precipitation series, subperiod 1861–1900. Note: stmod-ori, stmod-hom and grid-2 in mm, grid-1 in % of 1901–2000 average, stmod for the location 7.83 °E, 48.00 °N, grid-1 for 8 °E, 48 °N, grid-2 for 7.75 °E, 47.92 °N. Same scale for mm and % on the y-axis.

DOI: 10.1002/joc

A complete spatial compression to an average series over the entire GAR was not feasible because they would not be representative for any subregion, particularly for spatially variable elements like precipitation. To provide maximum information of a manageable size, we optimised the results of single-element regionalisations to a limited number of subregions that were identical for all climate elements. Regionalisation of each single element is based on principal component analysis (PCA) applied between all station records for the longest possible common period (approximately 1930 to 2000, with slight changes of a few years based on the availability of each element). The resulting empirical orthogonal functions (EOFs) were entered into an orthonormal transformation, which is subject to the so-called 'varimax-criterion' rotated empirical orthogonal functions, REOFs. Experience of our group from earlier attempts determined the way (Matulla *et al*., 2003) PCA was used (rotated EOFs) to investigate the spatial and seasonal variabilitiy of Austria's precipitation climate throughout the 20th century. REOFs were also used to regionalise the HISTALP temperature (Matulla *et al*., 2005) and the precipitation data set (Brunetti *et al*., 2005).

Here, we applied PCA to all available climate variables on an annual basis (normalised air pressure, air temperature, precipitation, cloudiness and sunshine duration data). Figure 8 shows the results. Regionalisation based on seasonal combinations (not shown) supports the annual results, but it also shows some interesting small-scale differences. The map presents the single-element regionalisations (thin lines) that are based on the four leading EOFs for each element, respectively. The loadings on all elements, except precipitation, also suggested a vertical stratification (e.g. a strong decoupling of lower and higher atmospheric levels is evident for winter temperature). Therefore, we introduced an additional subgroup for high-elevation summit sites. Stations within this Alpine subgroup are highly dispersed and are therefore not mapped as an area in Figure 8. For precipitation, the isolation of a specific high-elevation subgroup was not attempted owing to the exclusion of summit sites from the data set for this climate element (see earlier discussion in Section 3).

In order to allow comparisons between different climate elements, a regionalisation into uniform subregions (coarse resolution subregions – (CRSs)) that are the same for all climate elements was necessary. These CRSs (shown with bold lines in Figure 8) are semi-subjectively optimised solutions in order to gain the best possible common regions for all climate elements. In general, the adjustments of single-element regionalisations are considered to be small and physically reasonable. Most of the climate elements show a favourable subdivision into four horizontal subregions of approximately similar size. They correspond to the northwest–northeast–southwest–southeast scheme.

In detail, there were no compromises necessary along a section of the Central Alpine chains, from the La Grave–Les Écrins group in the West to the Hohe Tauern group in the East. This is the sharpest climate border existing in the GAR identical for all five elements. It is part of the continental scale transition zone, from the temperate westerly to the Mediterranean subtropical climate. Further to the west, this climate border splits into three branches. Two (for air pressure and temperature) bend to the south and continue to follow the Alpine bow a little further, whereas the other elements leave the Alpine crest and cross the Rhone valley in a zonal direction towards the Massif Centrale.

We see the strongest blurring of this divide in the zonal climate in the east. For cloudiness and sunshine, it bends to the south and generally follows the Dalmatian coast. For air pressure, it moves further inland and separates at the Dinaric Alps and Bosnian Mountains from the Slavonian–Hungarian plains. For temperature, it continues more or less in the zonal direction as it did in the Alpine

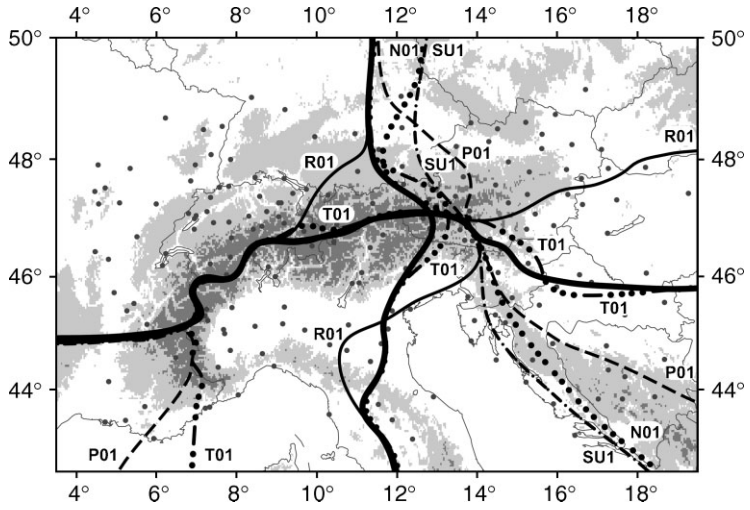

Figure 8. Leading horizontal climatological subregions of the GAR. Thin lines: results of PCA (based on single-element monthly anomalies) for air pressure, P01; air temperature, T01; precipitation, R01; sunshine, SU1; cloudiness, N01. Bold lines: the CRS (coarse resolution) compromise allowing for intra-elemental comparisons based on equal subregions for each climate element.

DOI: 10.1002/joc

parts. For precipitation, surprisingly, southern influences reach as far to the north as southern Slovakia. Here in the east, the strongest compromises had to be accepted to define a common CRS-border, which was finally chosen similar to the temperature line along the 46th parallel.

A second continental scale climate border could be anticipated between (western) oceanic influences of the Atlantic and (eastern) continental features of the Eurasian continent. Surprisingly, the climate transitions emerged to be rather uniform and steep for the different climate elements, although no additional topographic forcing through mountain chains exists here. They roughly follow the 12th degree eastern meridian in the parts of the GAR north of the Alps. In the south, a separate diversification along 12 °E appeared only for temperature and precipitation. This splitting into a southwestern 'Tyrrhenian' and a southeastern 'Adriatic' subregion is not visible for air pressure, sunshine and cloudiness. These three elements split into three horizontal subgroups only – most likely a stable solution for air pressure, and a preliminary estimate for sunshine and cloudiness owing to network deficiencies that still exist in parts of the GAR (see Section 2). Anyway, the subdivision into four horizontal subgroups was maintained also for these elements and a compromise between temperature and precipitation was followed in the south. This should cause no problems for pressure, cloudiness and sunshine – simply producing very similar respective SW- and SE-series – and the existing SW–SE differences for precipitation and temperature are not destroyed.

We finally chose four low-elevation coarse resolution subregions as shown in Figure 9(a). The fifth (high-elevation) subregion is indicated as a chain of triangles following the main crest-line of the Alps. The other three schematic graphs 9(b), 9(c) and 9(d) show the different combinations of subregions used in the following section. Together, ten subregions are defined as various combinations of the five main CRSs. Table III defines the wording and abbreviations used to denote the ten CRSs in the following section, these together outline the leading spatial features of climate variability in the GAR represented by the CRS mean time series (CRSMs). It also shows the starting years of each CRSM series. All low-elevation subregions of air pressure and temperature go back to the 18th century, and for precipitation to the year 1800. Sunshine series start in the 1880s, with some cloudiness subregional series starting earlier, in the 1840s and 1850s. The four low-elevation subregions for which humidity series are available point to the potential of this climate element that is not yet fully processed and used – neither in the GAR nor in most other regions of the world. Relative humidity series go back as far as the 1860s, those of vapour pressure go back even further in some cases. The reason vapour pressure is a longer series is that it is more easily homogenised compared to the more scattered relative humidity fields. The typical starting time of high-elevation series is in the 1860s to 1880s, when the classical Alpine summit observatories were founded (e.g. Wege, 2004; Eckert, 2004; Böhm, 2004; Auer *et al*., 2002).

For each of the ten CSRs, monthly, seasonal, half-year and annual CRSM series have been calculated for air pressure, air temperature, cloudiness and sunshine duration. Nine CRS sets of series could be produced for

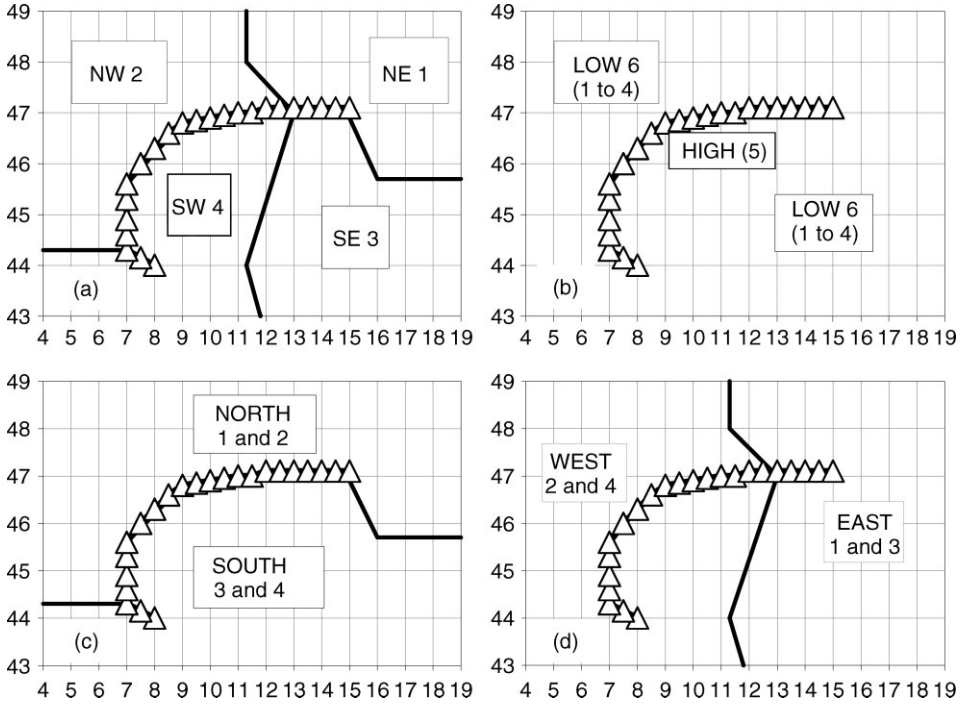

Figure 9. Schematic outlines of the coarse resolution subregions used: (a) horizontally defined subregions NE 1, NW 2, SE 3, SW 4, and their respective pairs of antagonistic combinations: (b) HIGH 5 and LOW 6 (combining 1,2,3,4), (c) NORTH (1,2) and SOUTH (3,4), (d) WEST (2,4) and EAST (1,3). Abscissa: E, ordinate: N.

DOI: 10.1002/joc

Table III. Codes, acronyms and names used for the coarse resolution subregions of the GAR.

HISTALP-CRSM-code				Starting years of CRSM series						
Code	Acr.	Combining	Subregion	Air-press.	Temp	Precip	Sun	Cloud	Rel-hum	Vap-press
1	NE		Northeast	1775	1767	1800	1880	1842	1860	1837
2	NW		Northwest	1760	1760	1800	1881	1864	1874	1874
3	SE		Southeast	1766	1767	1800	1884	1858	1860*	1845*
4	SW		Southwest	1763	1760	1800	1886	1858	n	n
5	H		High	1864	1818	n	1884	1878	1887	1881
6	L	1,2,3,4	Low	1775	1767	1800	1886	1864	n	n
7	N	1,2	North	1775	1767	1800	1881	1864	1874	1874
8	S	3,4	South	1766	1767	1800	1886	1858	n	n
9	W	2,4	West	1763	1760	1800	1886	1864	n	n
10	E	1,3	East	1775	1767	1800	1884	1858	n	n

* SE is represented by one series only.

precipitation (all except group 5) and four (NW, NE, H and N) for relative humidity and vapour pressure. The following section discusses a sample of typical and interesting cases from the total of more than 1000 single graphs that resulted from the reduction of the data sets to the few leading principal components.

Before presenting some interesting features of climate evolution based on the CRSM-concept, we want to clearly state the necessity to compress the information in order to reduce the otherwise unmanageable variability patterns; however, we must not forget that there remains a certain internal variability within the coarse resolution subregions. Therefore, any future analysis of pattern at a higher spatial resolution than the one chosen for this paper may be a valuable supplement to our comparative overview. To illustrate this, we have analysed the correlation (Spearman's correlation coefficient, described e.g. in Sachs, 1978) of all the station pairs within the subregions and plotted them relative to their separation distance. After grouping them according to inter-station distance, the medians of these subgroups were used to fit exponential spatial de-correlation functions. This was undertaken for all 5 CRSs, for all monthly, seasonal, semi-annual and annual CRSM series. Figures 10 and 11 show a selection of the graphs. They display 'box and whiskers' plots for the medians, and 4 percentiles of the group-samples and the exponential fits. Figure 10 demonstrates, with examples, the plots for January and July and subgroup 1 (NE), the intra-elemental differences and their annual variation. Figure 11 indicates the different de-correlation slopes in the different climate zones of the GAR with examples of four seasonal plots of the respective pairs of two contrasting subregions (NW vs. SW).

6. OUTLINE OF THE LEADING CLIMATE VARIABILITY FEATURES IN THE GAR

The HISTALP database achieved its present state in spring 2005. There has been no comprehensive study as yet making full use of its currently available potential. One study that deals with one single climate element has been undertaken. Brunetti *et al*. (2005) analysed the precipitation variability in the GAR on the basis of the HISTALP database released recently. Böhm *et al*. (2001) made use of an earlier version of the temperature data set with a lower station density and without any outlier correction. Detailed analyses of the other elements of the database have not yet been undertaken. The current potential of HISTALP is promising, as it makes possible an advanced physical understanding on long-term climate variability arising from comparative analysis of different climate elements over one to two centuries. In this final section we will touch on the different aspects that are worthy of a further closer examination.

Before starting to outline the features of climate variability during the instrumental period in the GAR, we want to particularly point to one of the strengths of the HISTALP data set that, at the same time, could also be one of its dangers if used uncritically. This pertains to the extension of HISTALP into the early instrumental period, for air pressure and temperature even by some decades into the 18th century. This opens interesting new possibilities to compare climate data from a highly natural period having a low level of anthropogenic interference with the recent period of combined anthropogenic and natural forcings. We have already mentioned this in the introduction and will come back to it several times in the following discussion. Users of these early data should be aware that the general quality level of the series during the last decades of the 18th century and the first two of the 19th does not match that of the recent parts of the instrumental period. However, considering the amount of work we had invested throughout the past decade and the lessons learned, we are convinced that our early homologous series is valuable when used with care. The network density in relation to spatial de-correlation (compare Figures 1, 3 and 10) has allowed quite important conclusions to be drawn for temperature, air pressure and precipitation for decades in which only indirectly derived climate information was available so far. As the series originate from different sources, institutes and administrations, we are also optimistic of the detection potential of systematic biases. The relatively small region provides

DOI: 10.1002/joc

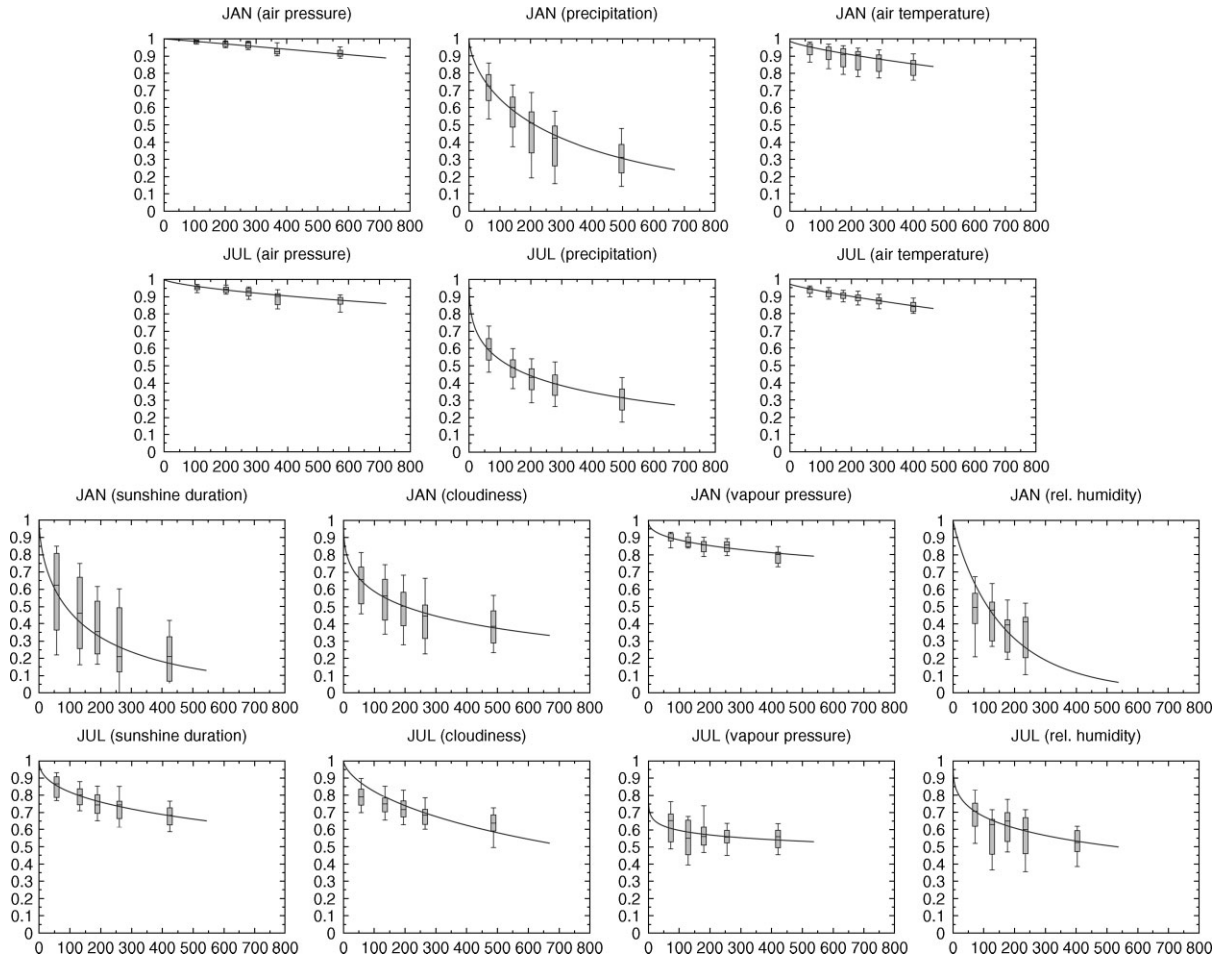

Figure 10. Spatial inter-station de-correlation within CRS 1 (NE) for the seven climate elements present in HISTALP for the months of January and July, respectively. Vertical axes, Spearman's correlation coefficient; horizontal axes, distance in km; boxes, medians, 75 and 25% percentiles; whiskers, 10 and 90% percentiles of inter-station-distance subgroups; lines, exponential de-correlation fits (calculated from the grouped data).

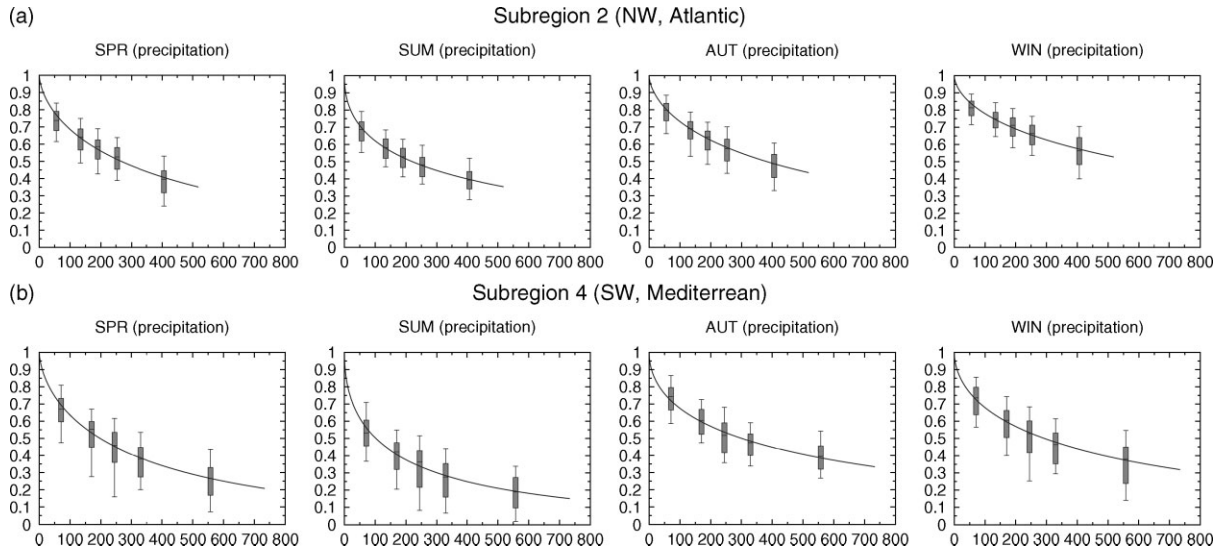

Figure 11. Spatial de-correlation for CRS 2 NW (a) and 4 SW (b) for precipitation and for the four seasons, respectively. SPR (MAM), SUM (JJA), AUT (SON) and WIN (DJF). Same layout as for Figure 10.

DOI: 10.1002/joc

at least 14 temperature series and six pressure series as early as 1781, which allow relative homogeneity testing to be undertaken. The advantages of systematically measured and intensively quality controlled time series now available for this period, in our opinion, compensates for the uncertainties that remain, although we are aware that objective measures to quantify this are not (and perhaps will never be) available owing to the absence of a standard definition of the 'ground truth' of the climate in those times.

6.1. Temperature

Although the following subsections will concentrate on the aspect of 'multiple variable climate', some introductory remarks on temperature are warranted, as this is the most frequently used single climate element in connection with climate change. The smoothed low-elevation subregional annual temperature series in Figure 12 clearly show that the GAR-subregions only show small differences in their low-frequency temperature variability. This is also the case for the high- *versus* low-elevation subgroups. The remote observatories in the Alpine summit, at altitudes of 1500 to 3500 m, all show the same long-term temporal evolution as those in the long-term urban or rural sites in the valleys and plains in and around the Alps. The mountains neither show weaker warming (which would point at the low-elevation sites to be possibly not representative for the global background) nor show any warming stronger than the low-elevation regions (as sometimes claimed, for example by Beniston *et al.* (1997) and others). It is the GAR as a whole that has warmed twice as much since the late 19th century compared to the global or Northern Hemispheric average (Figure 13). This has also been confirmed by a study of the independently homogenised Swiss series (Begert *et al.*, 2005) and Italian data (Brunetti *et al.*, 2006). The difference of the series in the GAR minus CRU-N-HEM shown in the upper part of Figure 13 further differentiates this relative trend. In the first years of the common measuring period (1850s and 1860s) and in the 80 years from 1900 to 1980 there is no trend between the GAR and the hemispheric average, and only a stronger variability of the GAR is visible (which is not surprising as the GAR is a smaller region). The long-term effect is produced more or less exclusively by a cool GAR in the 1870s, 1880s and 1890s in contrast to a warm GAR in the 1980s and 1990s. A discussion of such outstanding climate events at the decadal scale is fully described in Matulla *et al.* (2005) on the basis of the HISTALP database and cross-checked against long-term runs of climate models.

The pronounced seasonal differences in the long-term temperature evolution in the GAR are visible in the two upper series in Figure 14. The upper left graph shows the typical subdivision of the summer half-year series with more than 100 years of cooling prior to the 1910s followed by warming in two steps (until 1950 and in the recent decades). In the winter half-year, the initial cooling was much weaker and ended near 1890, with the 20th century warming being more regular and less steplike.

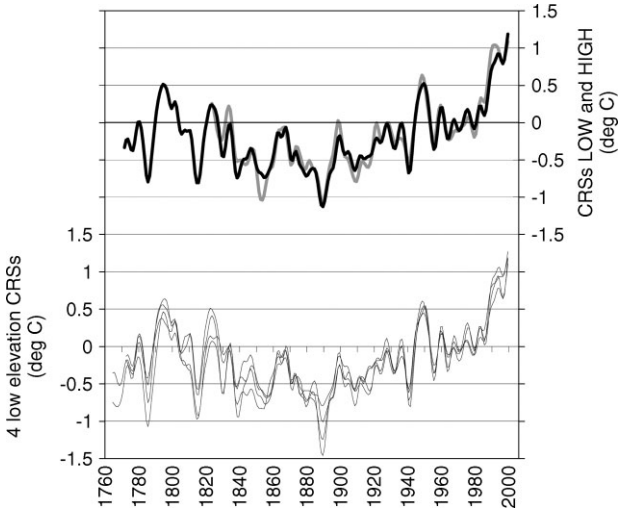

Figure 12. GAR smoothed temperature series 1760–2003 for the four low-elevation CRSs (bottom) and for the low-elevation mean (black) *versus* the high-elevation mean (grey, top). All values shown are 10-year Gaussian low-pass filtered anomalies from the 1901–2000 average.

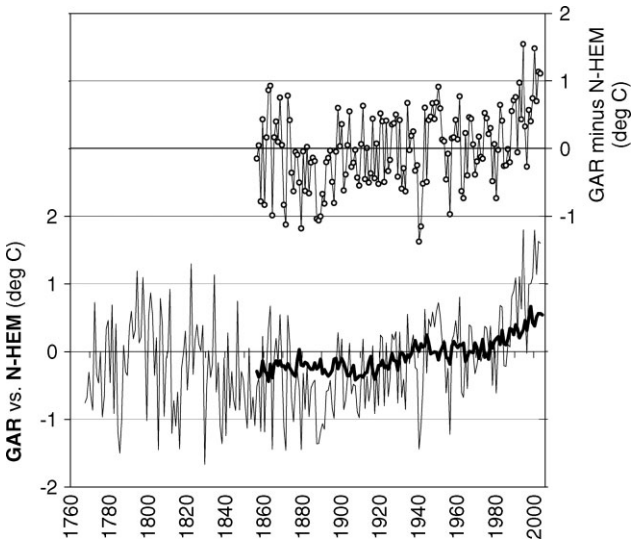

Figure 13. GAR-low elevation means compared to CRU-Northern-Hemisphere mean temperature series. Bottom (left ordinate): GAR-low 1767–2003 (thin) and CRU-N-HEM 1856–2003 (bold). Top (right ordinate): difference series GAR-low minus CRU-N-HEM. All values are anomalies from the 1901–2000 average.

6.2. Temperature and pressure

The main depiction in Figure 14 is the comparison of the respective low-elevation air pressure series. However, there is a striking similarity between the long-term trends of air temperature and air pressure. Figure 15(a) shows the 100- and 50-year trends of the annual data that have the same sign throughout the 19th and the 20th century. The spring, summer and autumn trends (Figure 15(b), (c), (d)) also show this similarity of pressure and temperature trends for most of the 50- and 100-year subperiods. Interestingly, winter temperatures seem to have been influenced differently by air pressure in the course of the past two centuries. In the 19th century, the temperature

DOI: 10.1002/joc

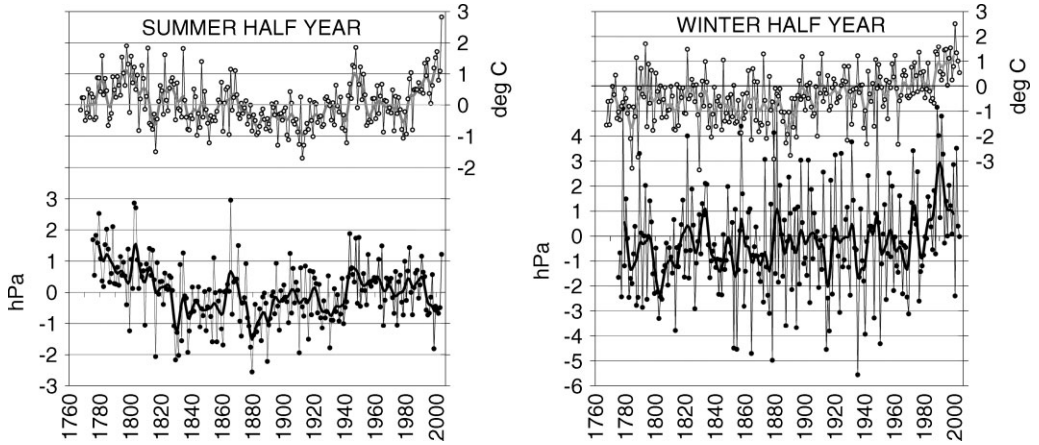

Figure 14. GAR-low: half-year mean temperature (grey, top) *versus* air pressure series (black, bottom), single years and 10-year low-pass filtered. Left graph: summer half-year (AMJJAS), right graph: winter half-year (ONDJFM). All values are anomalies from the 1901–2000 average.

trends are opposite to the trends of air pressure. This is in accordance with our traditional way of understanding Central European winters to be cold at high pressure, caused by an extension of the Asian winter anticyclone. In the 20th century, temperature and pressure trends increasingly tended to show the same sign rather than the opposite. This was most accentuated in the second part of the century, when a 4.5-hPa increase of winter air pressure went along with a 1.6-K warming. The uniform subregional pressure trends in the region (not shown in Figure 15 but included in Tables IV and V) point to the possibility that the increase in pressure do not necessarily have to be in connection with the continental East but may as well emerge from the South. Such a pattern, with reduced cyclonic activity during the Mediterranean winters, would enhance advection from the Atlantic and cause the observed warming of GAR-winters. It would also explain the observed centennial precipitation increase/decrease in the NW/SE of the Alps (Figure 19 and Tables IV and V).

The fact that each variable has been homogenised separately makes the described pressure–temperature similarities all the more remarkable. Moreover, the homogenised air pressure data also give more confidence to the early instrumental period in general and may also be used as a first simple explanation of some of the regional GAR *versus* global climate features. There is also some divergence of the air pressure and the temperature curves in Figure 14, for example, the recent decoupling of the summer curves since around 1990. Taking into account the problems of detecting and adjusting recent inhomogeneities (adjusting the necessary length of an unaffected subperiod is not possible for this period) and also the current conversion of the networks (automation), it may well be an artefact. Anyway this interesting feature should be kept under close observation during future updations.

Figure 16 highlights another aspect of the joint analysis of air pressure and air temperature. One of the strongest relationships between any pair of climate element combinations in the GAR is shown here. This is the one between high-elevation minus low-elevation difference in air pressure and air temperature series. The respective correlation coefficients are 0.89/0.87 for AMJJAS/ONDJFM. This is due to the thermodynamic expansion/compression of the warming/cooling air masses below the high-elevation observatories, producing an increase/decrease of high-altitude air pressure relative to the one measured at low elevations. The effect is not new, but its manifestation in long-term series is small in relation to the inhomogeneities present in the original data (Figure 5). A feasibility study (Böhm *et al.*, 1998) tried to use this approach to calculate the 'non thermometric virtual air temperature series' for air columns between some single high–low station pairs in the Eastern Alps. The model worked well for an annual 'Eastern Alpine Standard Air Column' temperature anomaly series. It confirmed the reality of the systematic bias in the 'as measured' temperature series (Figure 5) and also provided a striking argument against those who doubted the warming, not believing it to be real, and considering it only as an artefact of urbanisation. In the Alps (the only place where long-term series of high- and low-elevation air pressure exist at altitude differences of 2 to 2.5 km), the warming of the last 100 to 120 years calculated from the air pressure series corresponds exactly to that measured by homogenised long-term series from the urban and rural sites of the region. This is a clear indication that a possible 'systematic urban bias' cannot be used as an argument to doubt climate warming. It is obviously possible to eliminate urbanization problems through careful homogenising – an experience not only gained by the authors (comp. Böhm, 1998) but also by others (Peterson, 2003; Parker, 2004). A more sophisticated relevant study on 'barometric temperature series' (making use of the quantitatively enlarged and qualitatively improved database) is currently in progress.

6.3. Sunshine, clouds and precipitation

Figure 17 compares two climate elements expected to be closely inversely correlated – sunshine duration and cloudiness. Any similarities, however, are not as easy

DOI: 10.1002/joc

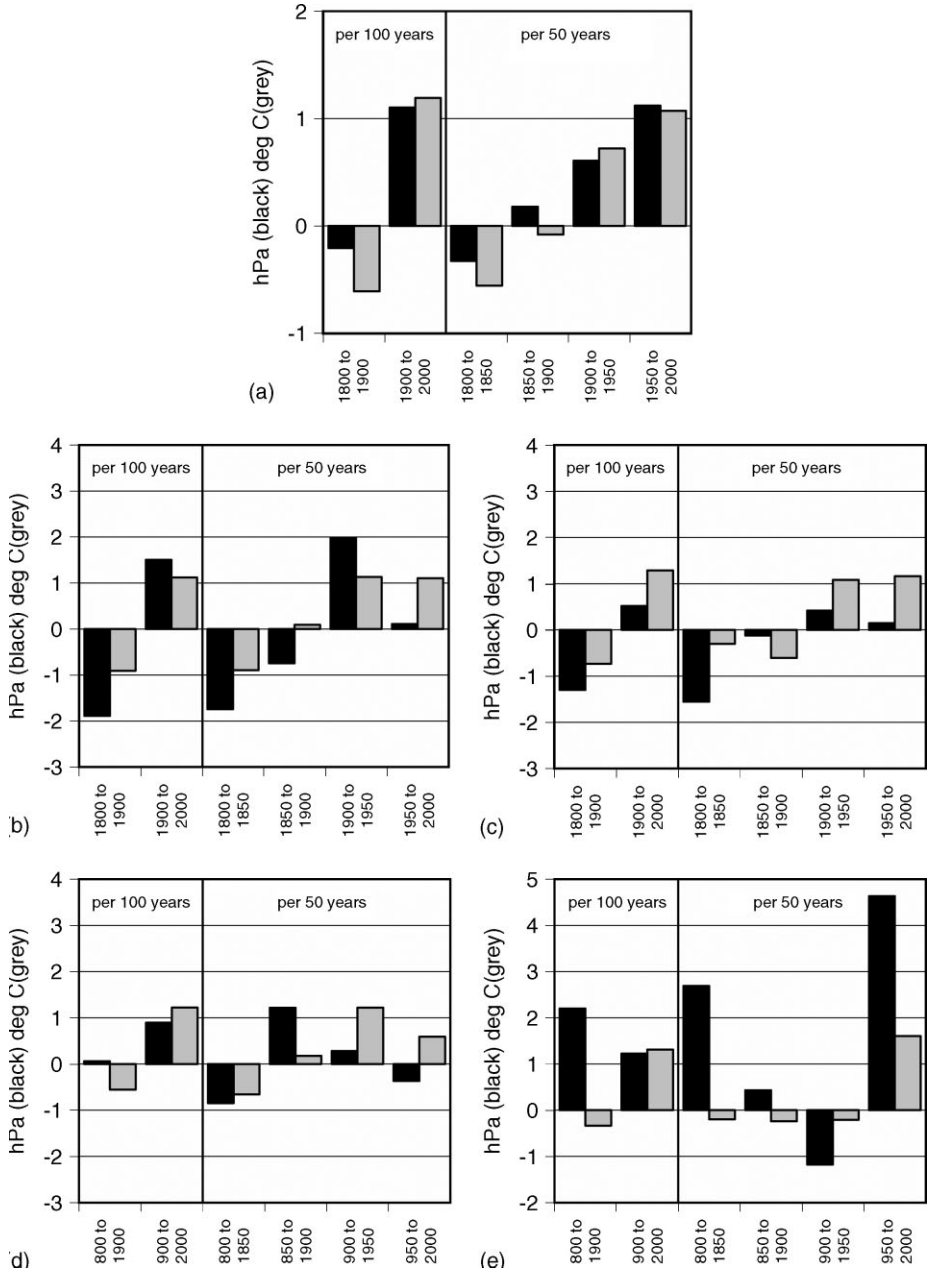

Figure 15. GAR-low: 100-year and 50-year linear trends of mean temperature (grey) and air pressure (black). 15(a) annual, 15(b) spring (MAM), 15(c) summer (JJA), 15(d) autumn (SON), 15(e) winter (DJF).

to determine as it may seem. Sunshine duration is measured as a total over a variable length of a day, whereas the sky coverage by clouds is estimated by an observer at fixed points in time each day. Also, the fact that the two elements have never been merged during the process of homogenisation (Section 3) makes results like the selected cases shown for the month of February in NW and for the month of May in SE rather satisfying. The inverse correlations of $-0.87/-0.79$ represent typical results and not specially selected examples. Figure 18 allows for a verification as it contains all the respective monthly correlations in the five coarse resolution subregions of the GAR, for sunshine-cloudiness as well as for the positively correlated pair of precipitation and cloudiness.

The annual precipitation and cloudiness series are shown in Figure 19 for the CRS series NW and SE. The increase in precipitation in the NW of the GAR over the last 140 years has its counterpart in a similar increase in sky coverage, while the long-term drying in the SE is accompanied by a decrease in cloudiness trend. The monthly correlation analysis (Figure 18) also shows slightly lower but still strongly significant correlations than those of the sunshine–cloudiness pair. For both cases, correlations are more distinct from March to October and slightly, but clearly, lower during November to February. In the cold season, the situation becomes more complicated owing to the frequent occurrence of a decoupling of low-elevation local (stable) air masses (accompanied by inversions and low stratiform clouds or

DOI: 10.1002/joc

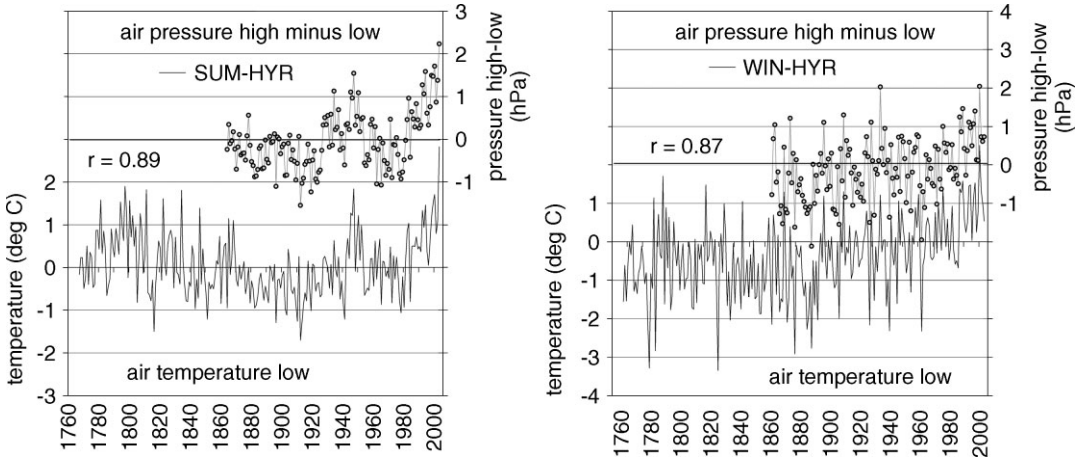

Figure 16. Seasonal air pressure difference series, high–low (grey) *versus* the mean low temperature series (black). Left graph, summer half-year (SUM-HYR = AMJJAS); right graph, winter half-year (WIN-HYR = ONDJFM). All values are anomalies from the 1901–2000 average.

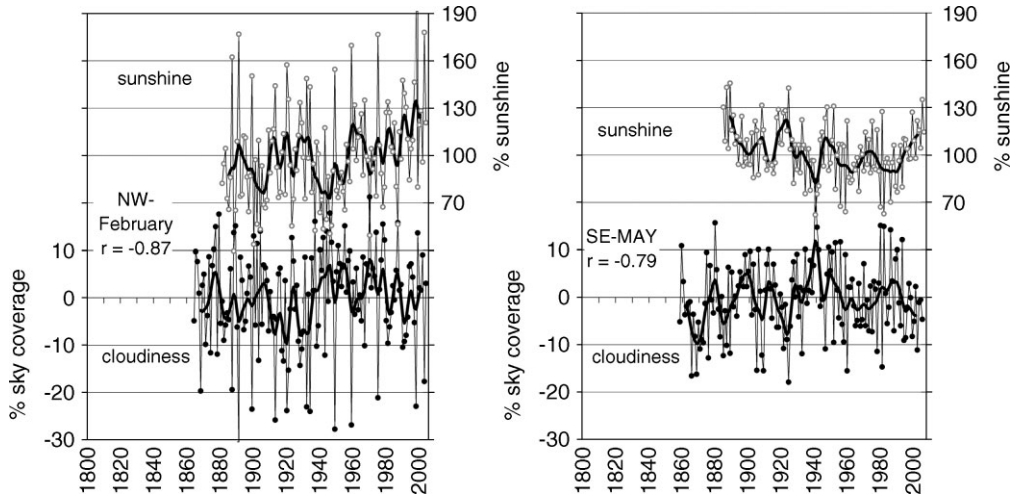

Figure 17. Examples for monthly sunshine (top) and cloudiness (bottom) series. Left graph, February; right graph, May. All values are anomalies from the 1901–2000 average, single months and 10-year low-pass filtered.

fog) from the higher parts of the atmosphere that are more exposed to advection from remote (maritime) regions. The existence of mountains with enclosed valleys and plains further stimulates and strengthens the decoupling in the cold season.

Figure 20 also serves to illustrate and argue in favour of such a mechanism that is driven by vertical effects. At first sight, the parallel long-term increase of winter precipitation and sunshine duration in subregion NW (left graph of Figure 20) seems to be inconsistent and appears to be an artefact of low data quality. A probable explanation is offered by the two cloudiness series observed at different altitudes in the right graph of Figure 20. At low elevations in the GAR, high averages of cloud-cover during winter result from long-lasting episodes of stratiform low-level clouds. These produce no, or very little, precipitation and completely shade the lower parts of the GAR from sunshine. However, they do not reach the altitudes of the high-elevation observatories. If these stratus episodes are broken by some frontal passages (in the north-western part of the

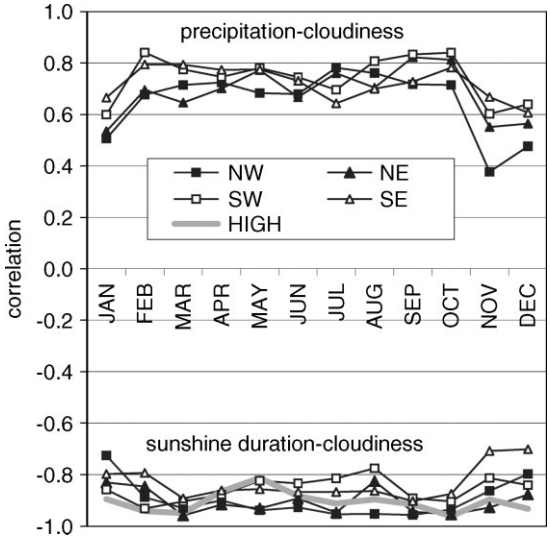

Figure 18. Monthly correlations between the pairs of climate elements (sunshine duration-cloudiness and precipitation-cloudiness) in the coarse resolution subregions of the GAR. Sample: 1901–2000.

DOI: 10.1002/joc

GAR typically advecting from the Atlantic) it brings rain or snow and increases the monthly total of sunshine hours. At high elevations (which have clear sky during the stratus-periods), above-normal frontal (precipitating) activity produces increased cloudiness (upper right graph of Figure 20). At low elevations the resulting effect of more high-level and less low-level clouds may produce a zero-result because there is only an exchange of one form of cloud against another form (lower right graph of Figure 20).

6.4. Relative humidity and vapour pressure

The last example selected from the bulk of information present in the HISTALP CRSM series deals with the two climate elements representing air humidity – relative humidity and vapour pressure. Although they are linked by a non-linear relation (the Magnus Equation), their (linearly calculated) monthly means have been treated in HISTALP as independent climate elements. Figure 21 confirms this and shows the different long-term evolutions of the two humidity measures. Of special interest is the comparison of the low- and the high-elevation humidity (shown in Figure 21 for CRS mean north) in combination with the respective temperature curves. The right graph in Figure 21 shows that vapour pressure has more or less simultaneously increased with temperature, both at high and low altitudes. This corresponds to the general simple line of argument that 'in a warmer world, there is more moisture in the atmosphere and precipitation is increased'. There is no doubt about this at the global scale. At the regional scale, on the other hand, the extent to which the humidity surplus can be transported from the (mainly oceanic) source regions into the continents is of fundamental importance. Yet the apparently nearly identical annual vapour pressure curves for high and low elevations of the GAR in the left graph (Fig. 21) have to be set into the context of the significantly lower water vapour content (in an absolute sense) of the (colder, less dense) high-elevation air masses. Thus, the identical 20th century increase of approximately 0.6 hPa tells

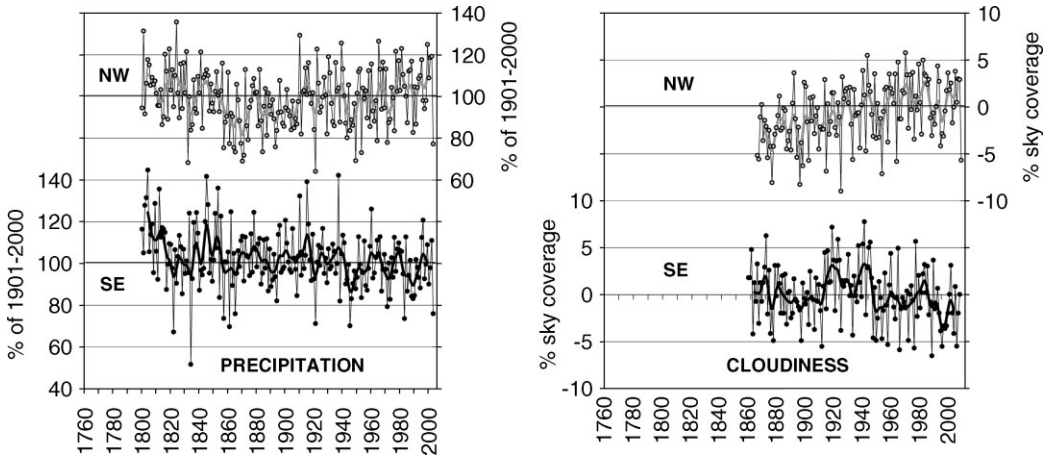

Figure 19. Left graph, annual precipitation series; right graph, annual cloudiness series. NW (top, grey) *versus* SE (bottom, black). All values relative to the 1901–2000 averages.

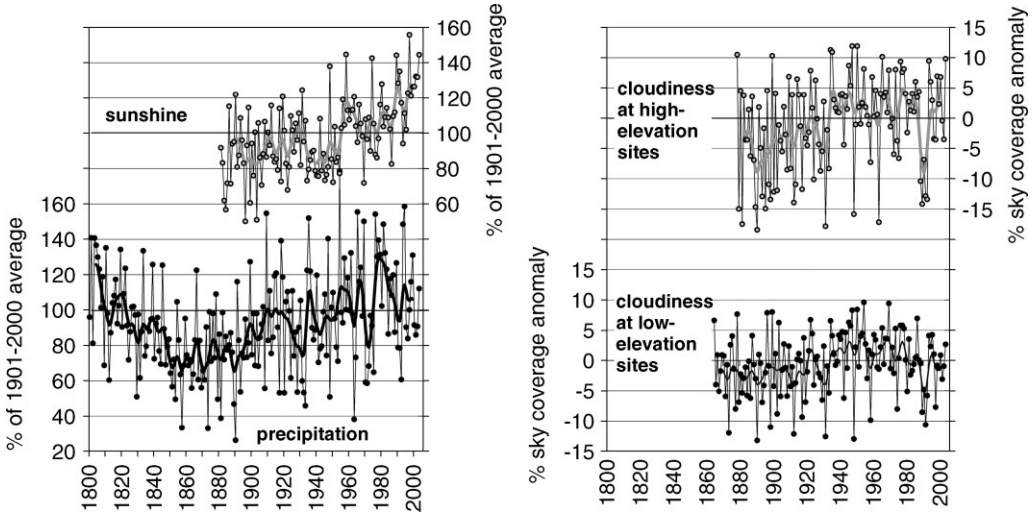

Figure 20. An (apparent) paradox. Left graph, low-elevation sunshine duration and precipitation (left) in NW-winters (DJF). Right graph, low- and high-elevation cloudiness in NW-winters (DJF). All values relative to the 1901–2000 averages, single years and 10-year low-pass filtered.

DOI: 10.1002/joc

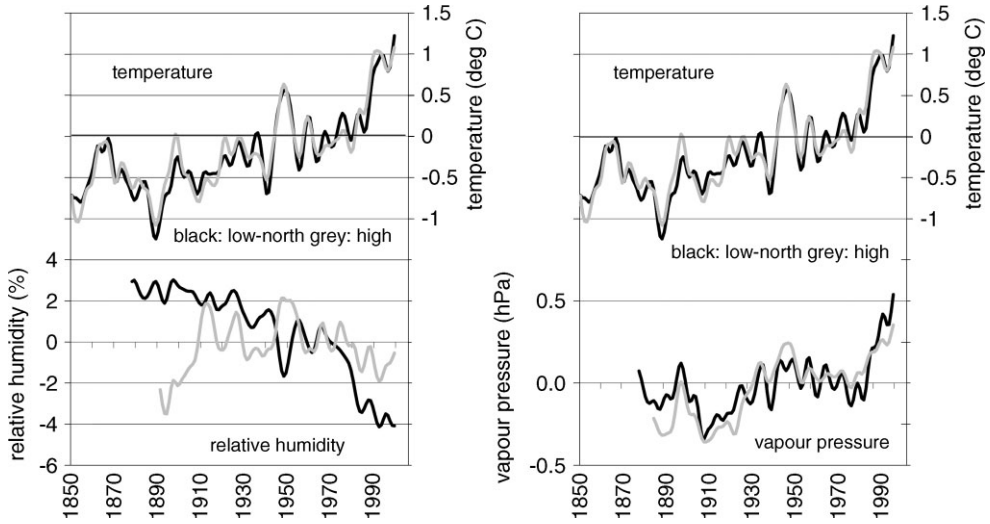

Figure 21. Annual relative humidity (bottom, left) and vapour pressure (bottom, right) compared to temperature (upper graphs, left and right). Black, low-elevation mean north (NW,NE); grey, high-elevation mean. All values are 10-year low-pass filtered anomalies to the 1901–2000 averages.

us about a more effective moisture transport towards the Alpine peaks compared to the less intensive one (in relative terms) into the valleys, basins and plains. This assumption is clearly supported by the long-term curves of relative humidity in the left graph of Figure 21. Here we see that, in the upper levels, the moisture transport is able to balance the drying potential of the warming trend happening equally at high and low altitudes. Over the whole measuring period, relative humidity has remained relatively stable in the mountains. Only a few oscillations at the decadal scale are visible, the most prominent being a dry period in the 1890s and early 1900s, which has its logical counterparts in a high-elevation decrease of vapour pressure and an increase of temperature. In the valleys, basins and plains, in contrast, a long-term decrease of relative humidity has occurred and it has steepened in recent decades. An outstanding period of interest is the one on the decadal scale in terms of the concurrent warming near 1950 at high and low altitudes, which was accompanied by a relative humidity minimum at low elevations and a moisture peak (for vapour pressure and relative humidity) at high elevations. This period seems to have been warm and dry in the lowlands but typically one of increased transport of convective moisture towards the elevated observatories in the high mountains. A similar effect is also visible for the recent warming of the 1980s and 1990s. The increase in low-elevation vapour pressure of approximately 0.5 hPa is not enough to balance the increase in temperature of more than 1 °C. Therefore, relative humidity has decreased considerably in the north low-elevation subregion. In contrast, the smaller increase of only 0.3 hPa in the high-elevation subgroup has to be set in the context of the (much lower) saturation vapour pressure in the colder air at high elevations. Therefore, this 0.3-hPa increase in the last 20 years was sufficient to keep relative humidity rather stable in the Alpine mountains.

6.5. Multiple-element trend overview

The selection of examples of interesting features illustrated and discussed in this section so far was intended to raise interest in the broad field of applications that was supported by the new HISTALP database. The selection is far from systematic and does not cover the whole spectrum of four-dimensional climate variability in the region. In Tables IV and V we outline a more systematic, but still compressed, GAR-overview of trends present in the annual/seasonal means/totals of the different climate elements. The tables show linear trends for fixed subperiods of 100, 50 and 25 years. To allow for comparisons with other regions and with global mean values we used the most common classification of the periods into centuries and half-centuries. The most recent half-century was again subdivided into two 25-year segments. The chosen subperiods also make sense in some respects in terms of major changes or reversals in climatic trend (e.g. the Atlantic Multi-decadal Oscillation). The two centennial subsections, for example, show a decrease in the 19th century in temperature (significant) and air pressure (not significant) and significantly increasing trends for both elements in the 20th century. The subdivision of the 19th century into two 50-year segments, on the other hand, is in accordance with a change in the mid 19th century, from decreasing precipitation in all subregions of the GAR to stable or increasing tendency in the second part. The stepwise increase in temperature in the 20th century is well described by using the 50-year segment from 1900 to 1950 (with significant warming in all subregions), and then the two subsequent 25-year section, with stable to slight (insignificant) cooling until the mid 1970s and the trend towards a strong warming of the recent 25 years.

The structure of the two tables (Table IV for annual, Table V for seasonal trends) also allows for quick geographical attribution. The left four trend values in each

DOI: 10.1002/joc

Table IV. Long-term annual climate trends in the coarse resolution subregions of the GAR in two 100-year, four 50-year and two (recent) 25-year subperiods. Trends have been calculated as linear regression coefficient multiplied by 10. Each box shows the trends in geographical order, bold figures mark 90% significance according to Mann–Kendall trend test, all values are decade^{-1} (mean trends in units 'per decade').

	ANNUAL TRENDS (JAN to DEC)																					
	Air pressure hPa			Temperature °C			Precipitation % of 1901–2000			Sunshine % of 1901–2000			Cloudiness % sky coverage			Vap. press. hPa			Rel. humidity %			
1800–1900	0.00	−0.06	–	**−0.05**	**−0.07**	–	**−1.9**	−0.6	–	–	–	–	–	–	–	–	–	–	–	–	–	100 years
	0.00	−0.02	−0.02	**−0.06**	**−0.08**	**−0.06**	−0.9	**−1.1**	**−1.1**	–	–	–	–	–	–	–	–	–	–	–	–	
1900–2000	**0.12**	**0.13**	**0.20**	**0.14**	**0.12**	**0.13**	**0.9**	**−0.8**	–	**0.5**	0.0	**1.2**	**0.25**	**−0.29**	**0.30**	**0.07**	**0.04**	**0.05**	**−0.11**	**−0.77**	−0.09	
	0.09	**0.09**	**0.11**	**0.13**	**0.10**	**0.12**	−0.1	**−0.9**	−0.2	**0.7**	0.0	0.3	0.09	**−0.33**	−0.10	–	**0.05**	–	–	**−0.83**	–	
1800–1850	0.01	−0.20	–	**−0.11**	**−0.16**	–	−1.3	−1.7	–	–	–	–	–	–	–	–	–	–	–	–	–	50 years
	−0.02	0.00	−0.06	−0.07	**−0.11**	**−0.11**	−1.5	**−2.9**	**−1.9**	–	–	–	–	–	–	–	–	–	–	–	–	
1850–1900	0.03	0.06	–	−0.04	−0.02	0.06	−0.7	**2.7**	–	–	–	–	–	−0.20	–	–	**0.07**	–	–	–	–	
	0.00	0.00	0.04	−0.02	0.00	−0.02	0.4	−0.4	0.7	–	–	–	–	–	–	–	0.05	–	–	–	–	
1900–1950	0.13	0.14	**0.31**	**0.19**	**0.12**	**0.18**	−0.4	−1.0	–	**1.3**	0.3	**3.1**	0.13	**−0.54**	0.30	**0.12**	**0.04**	**0.11**	−0.18	**−0.74**	0.25	
	0.09	0.12	0.12	**0.16**	**0.11**	**0.15**	−2.3	**−2.7**	−1.6	**1.6**	0.8	1.0	0.14	−0.13	−0.19	–	0.01	–	–	**−0.45**	–	
1950–2000	**0.20**	**0.25**	**0.45**	**0.25**	**0.21**	**0.24**	1.6	−0.6	–	−0.6	0.3	**1.2**	−0.10	−0.06	0.48	**0.11**	0.05	**0.04**	**−0.36**	**−1.30**	**−0.48**	
	0.23	**0.22**	**0.22**	**0.23**	**0.17**	**0.21**	−0.2	−0.5	0.1	−0.6	0.4	−0.1	−0.04	−0.36	−0.12	–	0.03	–	–	**−2.07**	–	
1950–1975	0.23	0.25	0.00	−0.04	0.05	−0.05	−1.7	−2.0	–	−2.1	−1.7	0.4	0.26	−0.21	0.13	−0.06	−0.01	−0.03	0.21	−0.25	−0.45	25 years
	0.18	0.25	0.22	−0.03	−0.07	−0.02	0.2	−2.0	−1.4	−0.9	−2.4	−1.8	−0.23	−0.02	−0.06	–	−0.02	–	–	**−1.47**	–	
1975–2000	0.17	0.27	**0.79**	**0.55**	**0.47**	**0.53**	0.5	3.3	–	**3.6**	**2.8**	2.9	−0.15	0.15	0.52	**0.36**	**0.25**	**0.15**	**−0.95**	**−1.47**	−0.35	
	0.26	0.25	0.23	**0.57**	**0.51**	**0.54**	−3.9	−0.8	−0.1	**3.4**	**4.8**	**3.7**	−0.35	**−1.35**	−0.24	–	**0.17**	–	–	**−2.29**	–	

SUBREGIONS: NW NE HIGH
CRSM-SCHEME SW SE LOW

DOI: 10.1002/joc

Table V. Long-term seasonal climate trends in the coarse resolution subregions of the GAR (layout and technical basis same as for Table IV). (a) MAM, (b) JJA, (c) SON, (d) DJF.

5a	**Spring Trends (MAM)**																					
	Air Pressure hPa			Temperature °C			Precipitation % of 1901–2000			Sunshine % of 1901–2000			Cloudiness % sky coverage			Vap. Press. hPa			Rel. Humidity %			
1800–1900	**−0.15**	**−0.22**	–	**−0.09**	**−0.10**	–	**−1.6**	1.1	–	–	–	–	–	–	–	–	–	–	–	–	–	100 years
	−0.21	**−0.21**	**−0.19**	**−0.10**	**−0.09**	**−0.09**	**2.2**	**2.7**	1.1	–	–	–	–	–	–	–	–	–	–	–	–	
1900–2000	**0.18**	**0.17**	**0.21**	**0.12**	**0.12**	**0.10**	1.1	−0.9	–	0.7	**0.9**	**1.4**	**0.44**	−0.08	**0.35**	**0.04**	0.02	**0.03**	−0.10	**−1.17**	0.04	
	0.13	**0.12**	**0.15**	**0.12**	**0.09**	**0.11**	−1.0	**−1.3**	−0.5	0.6	**0.9**	**0.7**	0.11	−0.19	0.08	–	0.04	–	–	**−1.39**	–	
1800–1850	−0.19	**−0.48**	–	−0.18	−0.19	–	−1.5	−2.4	–	–	–	–	–	–	–	–	–	–	–	–	–	
	−0.39	−0.29	−0.35	−0.18	−0.16	**−0.18**	**4.5**	5.8	1.4	–	–	–	–	–	–	–	–	–	–	–	–	
1850–1900	−0.14	−0.14	–	−0.02	0.06	0.04	−1.9	**4.8**	–	–	–	–	–	−0.21	–	–	**0.08**	–	–	–	–	50 years
	−0.18	−0.20	−0.15	−0.03	0.07	0.02	2.0	2.1	2.0	–	–	–	–	–	–	–	0.10	–	–	–	–	
1900–1950	0.39	**0.39**	**0.61**	**0.27**	**0.23**	**0.31**	−2.0	−3.4	–	**2.8**	2.8	**4.2**	−0.39	−0.73	−0.29	**0.11**	0.04	**0.11**	−0.31	**−1.26**	0.07	
	0.39	**0.42**	**0.40**	**0.23**	**0.17**	**0.23**	−2.3	**−6.5**	**−3.6**	**3.7**	**3.7**	**3.3**	−0.18	−0.22	−0.47	–	0.01	–	–	**−1.08**	–	
1950–2000	0.02	0.01	0.27	**0.21**	**0.27**	**0.21**	**4.7**	0.8	–	**−2.1**	−0.3	−0.2	0.78	0.38	**0.96**	**0.12**	0.08	0.03	−0.12	**−1.67**	**−0.41**	
	0.04	0.02	0.02	**0.20**	**0.20**	**0.22**	0.4	0.3	1.5	**−2.4**	0.5	−1.1	0.36	0.11	0.45	–	0.06	–	–	**−2.35**	–	
1950–1975	−0.64	**−0.72**	**−0.89**	−0.25	0.14	−0.23	6.7	1.1	–	**−8.7**	−3.9	−4.7	**3.61**	1.42	**2.29**	−0.08	0.02	−0.04	0.89	−0.77	0.30	25 years
	−0.66	**−0.63**	**−0.67**	−0.14	0.10	−0.04	4.5	2.3	3.6	**−6.3**	−2.0	−5.2	2.11	1.39	**2.11**	–	0.02	–	–	**−2.26**	–	
1975–2000	0.69	0.63	**1.36**	**0.87**	**0.61**	**0.74**	−1.9	4.4	–	**6.6**	2.0	**3.9**	−1.32	0.29	−0.32	**0.49**	**0.33**	**0.17**	**−1.24**	**−1.71**	−0.53	
	0.67	0.65	0.66	**0.81**	**0.50**	**0.70**	**−12.2**	−5.6	−3.9	**6.4**	**5.5**	**5.3**	−2.55	**−2.25**	**−0.91**	–	0.28	–	–	**−2.48**	–	
																SUBREGIONS:			**NW**	**NE**		**HIGH**
																CRSM-SCHEME			**SW**	**SE**		**LOW**

DOI: 10.1002/joc

Table V. (*Continued*).

5b	Summer Trends (JJA)																					
	Air Pressure hPa			Temperature °C			Precipitation % of 1901–2000			Sunshine % of 1901–2000			Cloudiness % sky coverage			Vap. Press. hPa			Rel. Humidity %			
1800–1900	**−0.10**	**−0.18**	–	**−0.07**	**−0.07**	–	−0.5	−0.6	–	–	–	–	–	–	–	–	–	–	–	–	–	100 years
	−0.10	**−0.15**	**−0.13**	**−0.09**	**−0.08**	**−0.08**	−0.9	**−2.1**	**−0.8**	–	–	–	–	–	–	–	–	–	–	–	–	
1900–2000	0.04	**0.11**	**0.17**	**0.14**	**0.13**	**0.13**	−0.4	−0.2	–	**−1.0**	**−0.8**	**0.8**	**0.34**	−0.15	**0.39**	**0.10**	**0.07**	**0.11**	−0.09	**−0.95**	**0.14**	
	0.02	0.03	0.05	**0.13**	**0.11**	**0.13**	1.0	0.5	0.2	**−0.8**	**−1.2**	**−0.9**	**0.35**	0.01	0.08	–	**0.10**	–	–	**−1.05**	–	
1800–1850	**−0.26**	**−0.46**	–	−0.06	−0.12	–	0.2	−0.4	–	–	–	–	–	–	–	–	–	–	–	–	–	
	−0.22	−0.19	**−0.31**	0.00	−0.04	−0.06	−1.4	**−4.0**	−0.9	–	–	–	–	–	–	–	–	–	–	–	–	
1850–1900	−0.03	−0.02	–	**−0.15**	**−0.11**	−0.11	−1.7	2.0	–	–	–	–	–	−0.24	–	–	**0.30**	–	–	–	–	50 years
	−0.04	−0.15	−0.02	**−0.12**	**−0.11**	**−0.13**	2.7	0.4	0.7	–	–	–	–	–	–	–	**0.17**	–	–	–	–	
1900–1950	0.07	0.15	**0.35**	**0.26**	**0.19**	**0.24**	−0.9	−0.6	–	0.2	−0.1	**3.5**	0.00	−0.65	−0.12	**0.19**	**0.08**	**0.24**	−0.08	**−0.65**	**0.47**	
	0.03	0.10	0.08	**0.23**	**0.19**	**0.21**	**−4.7**	−2.8	−2.3	0.6	−1.4	−0.2	−0.06	−0.35	−0.34	–	0.05	–	–	−0.47	–	
1950–2000	0.03	0.10	**0.26**	**0.28**	**0.22**	**0.22**	**−2.7**	−2.1	–	−0.9	0.1	**2.0**	−0.40	0.14	0.42	0.11	0.01	**0.05**	**−0.62**	**−2.10**	**−0.76**	
	−0.01	−0.02	0.03	**0.25**	**0.20**	**0.23**	−0.7	−0.1	−1.4	−1.0	0.4	−0.4	−0.02	0.18	−0.03	–	−0.03	–	–	**−2.63**	–	
1950–1975	0.20	0.18	−0.25	−0.16	−0.20	−0.26	−3.9	3.4	–	−3.5	−4.4	−2.4	0.00	1.07	0.86	−0.14	−0.06	−0.09	0.62	−0.39	0.59	25 years
	0.01	−0.01	0.11	−0.19	−0.37	−0.22	3.1	8.0	2.6	−2.6	**−5.4**	−3.9	−0.06	2.05	0.79	–	−0.08	–	–	−1.13	–	
1975–2000	−0.16	0.05	**0.66**	**0.68**	**0.73**	**0.70**	−0.6	1.5	–	3.0	**3.9**	**6.2**	−0.08	−0.51	0.10	**0.61**	**0.39**	**0.29**	**−1.30**	**−2.02**	**−1.22**	
	−0.15	−0.10	−0.08	**0.74**	**0.91**	**0.75**	−8.2	−6.5	−3.5	2.4	**6.6**	**3.9**	−0.60	**−2.32**	−0.69	–	**0.28**	–	–	**−3.78**	–	

SUBREGIONS: NW NE HIGH
CRSM-SCHEME SW SE LOW

Table V. (*Continued*).

5c	Autumn Trends (SON)																					
	Air Pressure hPa			Temperature °C			Precipitation % of 1901–2000			Sunshine % of 1901–2000			Cloudiness % sky coverage			Vap. Press. hPa			Rel. Humidity %			
1800–1900	0.01	−0.01	–	−0.04	**−0.08**	–	**−2.0**	**−1.8**	–	–	–	–	–	–	–	–	–	–	–	–	–	100 years
	0.03	0.01	0.01	**−0.05**	**−0.07**	**−0.05**	**−2.4**	**−2.4**	**−2.2**	–	–	–	–	–	–	–	–	–	–	–	–	
1900–2000	0.11	**0.10**	**0.21**	**0.15**	**0.12**	**0.15**	0.8	−1.2	–	**1.2**	0.4	**1.4**	0.08	−0.36	0.14	**0.07**	**0.06**	**0.04**	−0.04	**−0.41**	−0.10	
	0.07	0.07	0.09	**0.13**	**0.09**	**0.12**	0.1	−1.2	−0.4	**1.5**	0.3	**0.9**	−0.15	**−0.53**	−0.24	–	**0.08**	–	–	**−0.47**	–	
1800–1850	−0.11	−0.29	–	−0.11	**−0.20**	–	−0.3	−3.1	–	–	–	–	–	–	–	–	–	–	–	–	–	
	−0.07	−0.15	−0.17	−0.08	−0.14	−0.13	−3.9	−4.9	−3.3	–	–	–	–	–	–	–	–	–	–	–	–	
1850–1900	0.23	0.24	–	0.04	0.00	0.16	−0.1	2.0	–	–	–	–	–	−0.27	–	–	**0.12**	–	–	–	–	50 years
	0.25	**0.26**	0.24	0.05	0.04	0.04	−2.8	−4.2	−0.9	–	–	–	–	–	–	–	0.05	–	–	–	–	
1900–1950	0.09	0.03	0.33	**0.28**	**0.26**	**0.25**	1.5	−0.5	–	1.6	0.7	**2.6**	0.20	−0.51	0.42	**0.14**	**0.13**	**0.10**	−0.17	**−0.58**	0.51	
	0.05	0.05	0.06	**0.24**	**0.20**	**0.25**	−2.5	−1.0	−0.6	0.5	0.5	0.8	0.07	−0.26	−0.20	–	**0.15**	–	–	−0.06	–	
1950–2000	−0.10	−0.02	0.15	**0.16**	0.08	0.09	3.5	1.8	–	−1.1	−1.5	−0.5	0.24	0.71	**1.22**	0.09	0.04	0.05	−0.07	**−0.50**	−0.10	
	−0.10	−0.07	−0.07	**0.14**	0.08	0.12	2.9	2.4	2.7	0.1	−1.8	−1.1	0.55	0.19	0.48	–	0.02	–	–	**−1.56**	–	
1950–1975	0.28	0.20	0.03	−0.02	−0.06	−0.03	−1.2	−6.6	–	4.3	1.8	3.5	−1.50	−1.63	−1.03	−0.11	−0.09	−0.07	−0.40	−0.15	−0.98	25 years
	0.30	0.26	0.26	−0.08	−0.15	−0.08	−6.1	−3.3	−4.4	**4.3**	1.7	3.1	−1.73	−2.28	−1.71	–	−0.10	–	–	−1.16	–	
1975–2000	**−1.18**	−0.86	−0.56	**0.22**	0.23	−0.06	9.1	**11.1**	–	−1.9	−0.6	−4.2	1.93	**1.92**	**3.38**	**0.16**	0.13	0.11	−0.28	−0.79	1.14	
	−0.98	**−0.88**	**−0.99**	**0.27**	**0.36**	0.27	14.0	11.6	**11.4**	−1.4	−2.3	−1.7	3.02	1.67	**2.02**	–	0.08	–	–	**−1.66**	–	
																SUBREGIONS:			**NW**	**NE**		**HIGH**
																CRSM-SCHEME			**SW**	**SE**		**LOW**

DOI: 10.1002/joc

Table V. (*Continued*).

5d	Winter Trends (DJF)																					
	Air Pressure hPa			Temperature °C			Precipitation % of 1901–2000			Sunshine % of 1901–2000			Cloudiness % sky coverage			Vap. Press. hPa			Rel. Humidity %			
1800–1900	**0.20**	0.18	–	−0.02	−0.06	–	**−3.9**	**−1.9**	–	–	–	–	–	–	–	–	–	–	–	–	–	100 years
	0.26	**0.27**	**0.22**	−0.01	−0.06	−0.03	−1.9	−2.3	**−2.5**	–	–	–	–	–	–	–	–	–	–	–	–	
1900–2000	0.14	0.10	0.21	**0.16**	**0.11**	**0.15**	**2.4**	−1.1	–	**3.3**	−0.4	1.0	0.20	**−0.55**	**0.43**	**0.08**	0.01	**0.02**	**−0.23**	**−0.51**	**−0.34**	
	0.12	0.12	0.12	**0.15**	**0.11**	**0.13**	−0.2	−0.9	0.1	**2.4**	0.8	**1.5**	0.08	**−0.57**	−0.26	–	−0.01	–	–	**−0.47**	–	
1800–1850	**0.54**	0.46	–	−0.07	−0.12	–	**−7.0**	−4.2	–	–	–	–	–	–	–	–	–	–	–	–	–	
	0.60	**0.60**	**0.54**	0.05	0.02	−0.04	−4.5	**−10.1**	**−6.2**	–	–	–	–	–	–	–	–	–	–	–	–	
1850–1900	0.08	0.16	–	−0.08	−0.09	0.10	2.7	3.2	–	–	–	–	–	−0.19	–	–	**−0.20**	–	–	–	–	50 years
	−0.01	0.08	0.09	0.01	−0.04	−0.05	1.4	−0.1	2.0	–	–	–	–	–	–	–	**−0.16**	–	–	–	–	
1900–1950	−0.22	−0.19	−0.16	0.00	−0.10	−0.05	0.8	1.3	–	−0.3	**−5.5**	0.3	**1.04**	−0.04	**1.62**	0.04	−0.05	0.00	−0.11	**−0.36**	0.20	
	−0.29	−0.24	−0.24	−0.01	−0.06	−0.04	1.1	0.3	0.9	0.4	0.7	−1.2	**1.14**	0.57	0.53	–	−0.10	–	–	−0.07	–	
1950–2000	**0.86**	**0.90**	**1.15**	**0.41**	**0.31**	**0.46**	1.1	−2.8	–	**5.0**	**4.7**	**3.6**	**−0.97**	**−1.50**	−0.63	**0.14**	0.08	**0.05**	**−0.62**	**−0.94**	−0.57	
	0.98	**0.98**	**0.93**	**0.35**	0.23	**0.32**	−5.3	−5.0	−2.9	2.3	**4.2**	**4.0**	−1.00	**−1.87**	**−1.34**	–	0.07	–	–	**−1.83**	–	
1950–1975	1.40	**1.58**	**1.47**	0.41	0.41	0.51	−9.9	−9.0	–	5.4	3.7	6.8	−1.20	**−1.88**	−1.79	0.13	0.11	0.07	−0.46	0.13	−1.36	25 years
	1.36	**1.64**	**1.48**	0.36	0.19	0.36	0.3	−15.2	−8.7	3.1	−1.0	2.6	−1.32	−1.33	−1.52	–	0.13	–	–	**−1.88**	–	
1975–2000	1.37	1.38	**1.86**	**0.73**	0.58	**0.84**	−8.2	−8.7	–	**11.7**	**10.2**	**6.7**	−1.72	−1.61	−1.24	**0.24**	0.19	0.04	**−1.07**	**−1.31**	−0.76	
	1.68	1.44	1.47	**0.67**	0.45	**0.60**	**−17.6**	−10.1	**−10.9**	**9.4**	**10.5**	**10.5**	−1.52	−2.97	−1.85	–	0.12	–	–	**−1.93**	–	
																SUBREGIONS:			**NW**	**NE**		**HIGH**
																CRSM-SCHEME			**SW**	**SE**		**LOW**

DOI: 10.1002/joc

framed box are those of the low-elevation subregions NW (top-left), NE (top-right), SW (bottom-left) and SE (bottom-right). The two values in the right columns of each box are the high-elevation (top) and low-elevation trends. The tables provide quantitative information on many of the features already discussed in the examples given in the figures cited in this section. Key values (concerning the annual trends) are the −0.5 to −0.8 °C temperature decrease (significant in all subregions) in the 19th century and the subsequent 1.0 to 1.4 °C increase (also significant in all subregions) in the 20th century. Other cases of significant trends in all subregions are given for air pressure for the 20th century (increase of 0.9 to 1.3 hPa) and for the 50-years from 1950 to 2000, for temperature for both 50-year subsections of the 20th century and for the recent 25-year (all increasing), for vapour pressure (0.4 to 0.9 hPa increase in the recent 25 years) and for relative humidity with the drying of −1.8 to −10.4% from 1950 to 2000 (however, it has to be remembered that the two humidity elements are not available for all subregions).

Another outstanding event is the sharp trend-reversal for autumn-precipitation in the 1970s, from a long-term decreasing tendency (significant in the 19th century) to a sudden increase of 23 to 35% in the last 25 years (significant in the NE and for the low-elevation mean). A recent reverse is visible for winter. GAR-winters became drier in the last 25 years, significantly (44% in relation to the 20th century mean) in the SW and for the low-elevation mean (−27%). The recent trends in winter precipitation have been accompanied by respective trends in sunshine (significant increase in all subregions of 17 to 29%), cloudiness (non significant decrease of 3.1 to 7.4%) and relative humidity (significant decrease for all available low-elevation subregions, strongest in the SE with −4.8%).

Most of the other trends are variable from subregion to subregion. The element with the highest spatial variability of trends is precipitation. There is a 10% drying in the SW with an 8% wetting in the NE during the recent 25 years (annual totals). There is also a 10% drying in summer from 1950 to 1975 in the NW compared to the parallel 20% wetting in the SE, or the 16% decrease in long-term spring precipitation *versus* the contemporaneous increase in 27% spring precipitation during the 19th century.

For the other elements, some striking differences in trends exist between high and low elevations. For example, the centennial evolution of total sunshine in summer had a significant decrease (−9%) at low elevations, but a significant increase (+8%) at high elevations. Another 'vertical decoupling' is given for both 50-year segments and the 100-year trends of the 20th century for relative humidity in all four seasons. The decoupling is most pronounced in the more continental eastern subregions.

The indicated examples cover only a part of the information present in the two tables. Moreover, the idea of linear trend analysis for fixed subperiods only provides a restricted view on the full array of four-dimensional climate variability in the GAR. A more sophisticated respective analysis has already been undertaken for GAR-precipitation (Brunetti *et al*., 2005) and will be extended to all climate elements of the HISTALP database soon.

7. CONCLUSION AND OUTLOOK

The main objective of this paper was to introduce a new database, which is the result of approximately 10 years of data collection, digitising and quality improvement. The target area is the 'Greater Alpine Region', which is of special climatological interest owing to its location at the intersection of four principal climate regimes, and additionally modified by vertical effects. Our efforts were targeted at the elimination of shortcomings due to inadequate spatial coverage and resolution, exploitation of the data potential in the early instrumental period, followed by a multiple variable approach that was carried out under strict conditions with respect to data quality. To date, we succeeded in fulfilling these requirements for five leading climate elements at monthly resolution, but the database is in permanent development. The task for the future will be to continue the systematic high-resolution climate monitoring in the region with adherence to quality requirements. An extension of the database to other climate elements and an increase of the time resolution from monthly to daily are underway. In addition to these monitoring activities, we hope that the HISTALP database will be intensively used for climate variability analysis and for all kinds of climate impact research in the European Alps – a region of high vulnerability to climate change. Grid-1 data and CRSMs will be made available to the public via the ZAMG homepage (http://www.zamg.ac.at).

ACKNOWLEDGEMENTS

HISTALP was developed and systematically implied under the umbrella of the Austrian nationally funded project CLIVALP (Austrian FWF, P16076-N06). Further support came from a number of past and ongoing national and international projects ALPCLIM (EU, ENV4-CT97-06389), ALP-IMP (EU,EVK2-CT-2002-00148), ALOCLIM, (GZ. 308.938/3-IV/B3/96), CLIMAGRI (DM 484/7303/2000; DM 337/7303/2002; DM 639/7303/2003 e 504//7303/2000), CNR Special Project 'Reconstruction of the Past Climate in the Mediterranean area' (02-02/05/97-037681), the Swiss Projects KLIMA90 and NORM90, the Italian Meteorological Society project CLIMOVEST (Fondazione CRT) and the DHMZ and Croatian Ministry of Science Project 'Climate Variability and Change and Their Impacts' (0004003/2003).

We also want to express our appreciation for the work of two reviewers. Their remarks and corrections as well as our discussion with them considerably increased the value of our paper

REFERENCES

Aguilar E, Auer I, Brunet M, Peterson TC, Wieringa J. 2003. Guidelines on Climate Metadata and Homogenization. World

DOI: 10.1002/joc

Climate Programme Data and Monitoring WCDMP-No.53. WMO-TD No. 1186. WMO: Geneva.

Aschwanden A, Beck M, Häberli C, Haller G, Kiene M, Roesch A, Sie R, Stutz M. 1996. *Klimatologie der Schweiz*, *Heft 2: Bereinigte Zeitreihen. Die Ergebnisse des Projekts KLIMA90*, Band 1–4. Schweizerische Meteorologische Anstalt: Zürich.

Auer I. 1992. Precipitation measurements in a high alpine region–intercomparisons of different measuring systems. *TECO 92, WMO/TD* **462**: 251–256.

Auer I. 1993. Niederschlagsschwankungen in Österreich seit Beginn der instrumentellen Beobachtungen durch die Zentralanstalt für Meteorologie und Geodynamik. *Österreichische Beiträge zu Meteorologie und Geophysik*, Vol. 7. Zentralanstalt für Meteorologie und Geodynamik: Wien.

Auer I, Böhm R, Schöner W. 2001. Austrian long-term climate 1767–2000–Multiple instrumental climate time series from Central Europe. *Österreichische Beiträge zu Meteorologie und Geophysik*, Vol. 25. Central Institute for Meteorology and Geodynamics: Vienna.

Auer I, Böhm R, Leymüller M, Schöner W. 2002. Das Klima des Sonnblicks–Klimaatlas und Klimatographie der GAW Station Sonnblick einschließlich der umgebenden Gebirgsregion. *Österreichische Beiträge zu Meteorologie und Geophysik* **28**: 1–305.

Auer I, Böhm R, Scheifinger H, Ungersböck M, Orlik A, Jurkovic A. 2004. Metadata and their role in homogenising. *Proceedings of the Fourth Seminar for Homogenization and Quality Control in Climatological Databases*, WCDMP-No.56, WMO-TD No.1236. 17–23, WMO: Geneva, Budapest, Hungary, 6–10 October 2003.

Auer I, Böhm R, Jurkovic A, Orlik A, Potzmann R, Schöner W, Ungersböck M, Brunetti M, Nanni T, Maugeri M, Briffa K, Jones P, Efthymiadis D, Mestre O, Moisselin JM, Begert M, Brazdil R, Bochnicek O, Cegnar T, Gajic-Capka M, Zaninovic K, Majstorovic Z, Szalai S, Szentimrey T, Mercalli L. 2005. A new instrumental precipitation dataset for the Greater Alpine Region for the period 1800–2002. *International Journal of Climatology* **25**: 139–166.

Baudenbacher M. 1997. Homogenisierung langer Klimareihen, dargelegt am Beispiel der Lufttemperatur. *Veröffentlichung der Schweizerischen Meteorologischen Anstalt*,Vol. 58. Schweizerische Meteorologische Anstalt: Zürich.

Begert M, Schlegel T, Kirchhofer W. 2005. Homogeneous Temperature and Precipitation Series of Switzerland from 1864 to 2000. *International Journal of Climatology* **25**: 65–80.

Begert M, Seiz G, Schlegel T, Musa M, Baudraz G, Moesch M. 2003. *Homogenisierung von Klimamessreihen der Schweiz und Bestimmung der Normwerte 1961-1990. Schlussbericht des Projekts NORM90*,Vol. 67. Veröffentlichung der MeteoSchweiz: MeteoSchweiz, Zürich.

Beniston M, Diaz HF, Bradley RS. 1997. Climatic change at high elevation sites: an overview. *Climatic Change* **36**: 233–251.

Böhm R. 1992. Lufttemperaturschwankungen in Österreich seit 1775. *Österreichische Beiträge zu Meteorologie und Geophysik*, Vol. 5. Zentralanstalt für Meteorologie und Geodynamik: Wien. 1–96.

Böhm R. 1998. Urban bias in temperature time series–A case study for the city of Vienna, Austria. *Climatic Change* **38**: 113–128.

Böhm R. 2004. Die bergstationen obir und villacher Alpe: Eineinhalb jahrhunderte klimamessung und–beobachtung in den Südalpen. *Jahresbericht des Sonnblick Vereines* **100**: 52–53.

Böhm R, Auer I, Hagen M, Schöner W. 1998. Long alpine barometric pressure series in different altitudes as a measure for the 19th/20th century warming. *Proceedings of the 8thConference on Mountain Meteorology*. American Meteorological Society: Flagstaff, AZ; 72–76, 3–7 August 1998.

Böhm R, Auer I, Brunetti M, Maugeri M, Nanni T, Schöner W. 2001. Regional temperature variability in the European Alps 1760–1998 from homogenized instrumental time series. *International Journal of Climatology* **21**: 1779–1801.

Bosshard W. 1996. Homogenisierung klimatologischer Zeitzreihen, dargelegt am Beispiel der relativen Sonnenscheindauer. *Veröffentlichung der Schweizerischen Meteorologischen Anstalt*, Vol. 57. Schweizerische Meteorologische Anstalt: Zürich.

Brunet M, Saladié O, Jones P, Sigró J, Moberg A, Aguilar E, Walther A, Lister D, López D. 2006. The development of a new daily adjusted temperature dataset for Spain (1850–2003), *International Journal of Climatology*, Published online in Wiley InterScience (www.interscience.wiley.com) DOI: 10.1002/joc 1338.

Brunetti M, Buffoni L, Maugeri M, Nanni T. 2000. Trends of minimum and maximum daily temperatures in Italy from 1865 to 1996. *Theoretical And Applied Climatology* **66**: 49–60.

Brunetti M, Maugeri M, Monti F, Nanni T. 2006. Temperature and precipitation variability in Italy in the last two centuries from homogenised instrumental time series. *International Journal of Climatology* **26**: 345–381.

Brunetti M, Maugeri M, Nanni T, Auer I, Böhm R, Schöner W. 2005. Precipitation variability and changes in the Greater Alpine region over the 1800–2003 period. *Journal of Geophysical Research* 111, D 11107, DOI: 10.1029/2005/D06674.

Buffoni L, Maugeri M, Nanni T. 1999. Precipitation in Italy from 1833 to 1996. *Theoretical And Applied Climatology* **63**: 33–40.

Craddock JM. 1979. Methods of comparing annual rainfall records for climatic purposes. *Weather* **34**: 332–346.

Eckert W. 2004. Die Wetterstation auf dem Säntis. *Jahresbericht des Sonnblick Vereines* **100**: 40–42.

Efthymiadis D, Jones PD, Briffa K, Auer I, Böhm R, Schöner W, Frei C, Schmidli J. 2006. Construction of a 10-min-gridded precipitation dataset for the Greater Alpine region 1800–2003. *Journal of Geophysical Research* **111**: D01105, DOI:10.1029/2005 JD006120, 2006.

Forland EJ, Hanssen-Bauer I. 2000. Increased precipitation in the Norwegian Arctic: True or False? *Climatic Change* **46**: 485–509.

Frich P, Alexandersson H, Ashcroft J, Dahlström B, Demarée GR, Drebs A, van Engelen AFV, Førland EJ, Hanssen-Bauer I, Heino R, Jónsson T, Jonasson K, Keegan L, Nordli PO, Schmidt T, Steffensen P, Tuomenvirta H, Tveito OE. 1996. North Atlantic Climatological Dataset (NACD Version 1)–Final Report. Scientific Report, 96–1. Copenhagen Danish Meteorological Institute.

Gajić-Čapka M, Zaninović K. 1997. Changes in temperature extremes and their possible causes at the SE boundary of the Alps. *Theoretical And Applied Climatology* **57**: 1–2, 89–94.

Gisler O, Baudenbacher M, Bosshard W. 1997. Homogenisierung schweizersicher klimatologischer Messreihen des 19. und 20. Jahrhunderts. Projektschlussbericht im Rahmen des nationalen Forschungsprogrammes, Klimaänderung und Naturkatastrophen "NFF31.vdf Hochschulverlag an der ETH.

Groisman PYa, Legates DR. 1994. The accuracy of United States precipitation data. *Bulletin of the American Meteorological Society* **75**: 215–227.

Herzog J, Müller-Westermeier G. 1997. In Homogenization of various climatological parameters in the German weather service. *Proceedings of the First Seminar for Homogenisation of Surface Climatological Data*. Budapest, 6–12 Oct. 1996: 101–111.

Herzog J, Müller-Westermeier G. 1998. Homogenitätsprüfung und homogenisierung klimatologischer meßreihen im deutschen wetterdienst. *Berichte des Deutschen Wetterdienstes*, Vol. 202. Selbstverlag des Deutschen Wetterdienstes: Offenbach am Main.

Hungarian Meteorological Service. 1997. *Proceedings of the First Seminar for Homogenisation of Surface Climatological Data*. Készült a MET-DRUCK nyomdában: Budapest, 6–12 Oct. 1996.

Karl TR, Diaz HF, Kukla G. 1988. Urbanization: Its detection and effect in the United States climate record. *Journal of Climate* **1**: 1099–1123.

Likso T. 2004. Inhomogeneities in Temperature Time Series in Croatia. *Hrvatski meteorološki časopis (Croatian Meteorological Journal)* **38**: 3–9.

Matulla C, Penlap EK, Haas P, Formayer H. 2003. Comparative analysis of spatial and seasonal variability: Austrian precipitation during the 20th century. *International Journal of Climatology* **23**: 1577–1588.

Matulla C, Auer I, Böhm R, Ungersböck M, Schöner W, Wagner S, Zorita E. 2005. Outstanding past decadal-scale climate events in the Greater Alpine region analysed by 250 years data and model runs. GKSS-Report 2005/4. GKSS Forschungszentrum in der Helmholtz Gemeinschaft, Geesthacht.

Maugeri M, Nanni T. 1998. Surface air temperature variations in Italy: recent trends and an update to 1993. *Theoretical And Applied Climatology* **61**: 191–196.

Milkovi' J. 1989. Preliminary results of the WMO field intercomparison in Yugoslavia. Sevruk B (ed.). *Precipitation Measurement Workshop on Precipitation Measurement*. ETH Zurich: St. Moritz, 145–149.

Milkovi' J. 2002. Some results of the WMO intercomparison in Croatia; WCRP workshop on determination of solid precipitation in cold climate regions fairbanks, Alaska–June 9–14, 2002, CD.

Parker DE. 2004. Large scale warming is not urban. *Nature* **432**: 290.

Peterson TC. 2003. Assessment of urban versus rural in situ surface temperatures in the contiguous United States: no difference found. *Journal of Climate* **16**: 2941–2959.

Peterson TC, Easterling DR, Karl TR, Groisman P, Auer I, Böhm R, Plummer N, Nicholis N, Torok S, Vincent L, Tuomenvirta H, Salinger J, Förland EJ, Hanssen-Bauer I, Alexandersson H, Jones P, Parker D. 1998. Homogeneity adjustments of in situ climate data: A review. *International Journal of Climatology* **18**: 1493–1517.

Plummer N, Lin Z, Torok S. 1995. Trends in the diurnal temperature range over Australia since 1951. *Atmospheric Research* **37**: 79–86.

Potzmann R. 1999. Data Control and Visualisation with a Desktop GIS. *Proceedings of 2nd International Conference on Experiences with Automatic Weather Stations ICEAWS 1999, 27 to 29 September 1999, Vienna, Austria. Österreichische Beiträge zu Meteorologie und Geophysik*, Vol. 20. Central Institute for Meteorology and Geodynamics: Vienna, Austria, CD-ROM.

Sachs L. 1978. *Angewandte Stastistik–Statistische Methoden und ihre Anwendungen*. Springer Verlag: Berlin, Heidelberg New, York.

Schwarb M. 2000. The Alpine precipitation climate. Evaluation of a high-resolution analysis scheme using comprehensive rain-gauge data. PhD thesis **13911**: 1–131. Swiss Federal Institute of Technology (ETH), Zurich, Switzerland.

Schwarb M, Daly C, Frei C, Schär C. 2001. Mean annual and seasonal precipitation throughout the European Alps 1971–1990. In *Hydrologischer Atlas of Switzerland. Landeshydrologie und Geologie*, Sperafico R, Weingartner R, Leibundgut C (eds). Institute of Geography of University Bern: Switzerland, Plates 2.6 and 2.7.

Sevruk B (ed.). 1986. Corrections of precipitation measurements. *WMO/IAHS/ETH Workshop on Correction of Precipitation Measurements. Zürich, Switzerland, 1–3 Apr. 1985.* Swiss Federal Institute of Technology: ETH Zentrum. Zürich.

Szalai S, Szentimrey T. 2001. Does the climate warm in the 20th century in Hungary? Proceedings of the scientific session for the centenarium of the birth of Dr. sen. Dénes Berényi. Editor: Dr. Gábor Szász, DU-HAS-HMS.

Vincent LA, Zhang X, Bonsal BR, Hogg WD. 2002. Homogenisation of daily temperatures over Canada. *Journal of Climate* **15**: 1322–1334.

Wege K. 2004. Das Observatorium auf der Zugspitze. *Jahresbericht des Sonnblick Vereines* **100**: 29–33.

World Meteorological Organization. 1999. *Proceedings of the Second Seminar for Homogenisation of Surface Climatological Data. WCDMP 41, WMO-TD 962*. WMO: Geneva. Budapest, 9–13 Nov. 1998.

World Meteorological Organization. 2004. *Fourth Seminar for Homogenization and Quality Control in Climatological Databases. WCDMP 56, WMO-TD 1236*. WMO: Geneva, (Budapest, Hungary, 6–10 October 2003).

Yang D, Elomaa E, Gunther T, Golubev V, Goodison BE, Sevruk B, Madsen H, Milkovic J. 1999a. Wind-induced precipitation undercatch of the Hellmann gauges. *Nordic Hydrology* **30**: 57–80.

Yang D, Goodison BE, Metcalfe JR, Louie P, Leavesley G, Emerson D, Golubev V, Elomaa E, Gunther T, Hanson CL, Pangburn T, Kang E, Milkovic J. 1999b. Quantification of precipitation measurement discontinuity induced by wind shields on national gauge. *Water Resources Research* **35**(2): 491–508.

Zaninović K, Gajić-Čapka M. 2000. Changes in components of the water balance in the Croatian Lowlands. *Theoretical and Applied Climatology* **65**: 1–2, 111–117.

DOI: 10.1002/joc